US009464883B2

(12) **United States Patent**
Swanson et al.

(10) **Patent No.: US 9,464,883 B2**
(45) **Date of Patent: Oct. 11, 2016**

(54) **INTEGRATED OPTICAL COHERENCE TOMOGRAPHY SYSTEMS AND METHODS**

(71) Applicant: **ACACIA COMMUNICATIONS INC.**, Maynard, MA (US)

(72) Inventors: **Eric Swanson**, Maynard, MA (US); **Christopher Doerr**, Maynard, MA (US)

(73) Assignee: **Eric Swanson**, Gloucester, MA (US)

(*) Notice: Subject to any disclaimer, the term of this patent is extended or adjusted under 35 U.S.C. 154(b) by 0 days.

(21) Appl. No.: **14/201,827**

(22) Filed: **Mar. 8, 2014**

(65) **Prior Publication Data**

US 2014/0376000 A1 Dec. 25, 2014

Related U.S. Application Data

(60) Provisional application No. 61/838,313, filed on Jun. 23, 2013.

(51) **Int. Cl.**
G01B 9/02 (2006.01)

(52) **U.S. Cl.**
CPC ***G01B 9/02091*** (2013.01); ***G01B 9/02004*** (2013.01); ***G01B 9/02051*** (2013.01)

(58) **Field of Classification Search**
CPC G01B 9/02051; G01B 9/02091; G01B 2290/70; G01B 9/02002; G01B 9/02004; G01B 9/02005
See application file for complete search history.

(56) **References Cited**

U.S. PATENT DOCUMENTS

5,321,501 A 6/1994 Swanson et al.
5,459,570 A 10/1995 Swanson et al.
5,465,147 A 11/1995 Swanson
5,956,355 A 9/1999 Swanson
6,134,003 A 10/2000 Tearney et al.
6,160,826 A 12/2000 Swanson
6,191,862 B1 2/2001 Swanson et al.
6,288,784 B1 9/2001 Hitzenberger
6,445,939 B1 9/2002 Swanson et al.
6,485,413 B1 11/2002 Boppart et al.
6,501,551 B1 12/2002 Tearney et al.
6,564,087 B1 5/2003 Pitris et al.
6,891,984 B2 5/2005 Petersen et al.
7,061,618 B2 6/2006 Atia
(Continued)

OTHER PUBLICATIONS

D. Huang, E. A. Swanson, C. P. Lin, J. S. Schuman, W. G. Stinson, W. Chang, M. R. Hee, T. Flotte, K. Gregory, C. A. Puliafito, and J. G. Fujimoto, "Optical coherence tomography," Science, vol. 254, No. 5035, pp. 1178-1181, Nov. 1991.
(Continued)

Primary Examiner — Michael A Lyons
(74) *Attorney, Agent, or Firm* — Kurt Rauschenbach; Rauschenbach Patent Law Group, LLC

(57) **ABSTRACT**

Disclosed herein are optical integration technologies, designs, systems and methods directed toward Optical Coherence Tomography (OCT) and other interferometric optical sensor, ranging, and imaging systems wherein such systems, methods and structures employ tunable optical sources, coherent detection and other structures on a single or multichip monolithic integration. In contrast to contemporary, prior-art OCT systems and structures that employ simple, miniature optical bench technology using small optical components positioned on a substrate, systems and methods according to the present disclosure employ one or more photonic integrated circuits (PICs), use swept-source techniques, and employ a widely tunable optical source(s).

18 Claims, 36 Drawing Sheets

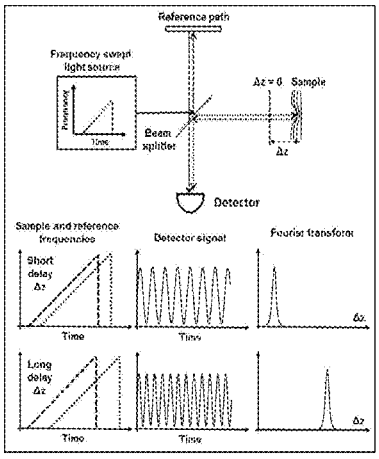

Example Specifications

- Center Wavelength ~ 1310 nm
- Scan Range > 100 nm
- Coherence Length > 20 mm
- Sweep Speed > 100 kHz
- Laser Output Power > 25 mW
- Ideal sweep 100% duty cycle sawtooth

(56) **References Cited**

U.S. PATENT DOCUMENTS

7,530,948	B2	5/2009	Seibel et al.	
7,864,822	B2	1/2011	Bouma et al.	
7,916,387	B2	3/2011	Schmitt	
8,078,245	B2	12/2011	Daly et al.	
8,384,909	B2	2/2013	Yun	
8,416,818	B2	4/2013	Bouma	
8,437,007	B2	5/2013	Flanders	
8,515,221	B2	8/2013	Flanders	
8,711,364	B2	4/2014	Brennan et al.	
8,947,648	B2	2/2015	Swanson et al.	
8,994,954	B2	3/2015	Atia et al.	
9,008,142	B2	4/2015	Minneman et al.	
2003/0223673	A1*	12/2003	Garito et al.	385/14
2010/0178056	A1*	7/2010	Liu	398/65
2012/0224165	A1	9/2012	Swanson	
2012/0226118	A1*	9/2012	Delbeke et al.	600/316
2012/0250007	A1*	10/2012	Na et al.	356/73.1
2013/0209022	A1	8/2013	Doerr	
2014/0147079	A1	5/2014	Doerr et al.	
2014/0203175	A1*	7/2014	Kobrinsky et al.	250/214.1
2014/0376001	A1	12/2014	Swanson	

OTHER PUBLICATIONS

Bernhard Baumann, WooJhon Choi Benjamin Potsaid, David Huang, Jay S. Duker, and James G. Fujimoto, "Swept source / Fourier domain polarization sensitive optical coherence tomography with a passive polarization delay unit", Optics Express, vol. 20, Issue. 9, Apr. 23, 2012.

R. Huber, M. Wojtkowski, J. G. Fujimoto, J. Y. Jiang, and A. E. Cable, "Three-dimensional and C-mode OCT imaging with a compact, frequency swept laser source at 1300 nm," Optics Express 13(26), 10523-10538 (2005).

R. Huber, M. Wojtkowski, K. Taira, J. G. Fujimoto, and K. Hsu, "Amplified, frequency swept lasers for frequency domain reflectometry and OCT imaging: design and scaling principles," Optics Express 13(9), 3513-3528 (2005.

B. Potsaid, I. Gorczynska, V. J. Srinivasan, Y. L. Chen, J. Jiang, A. Cable, and J. G. Fujimoto, "Ultrahigh speed spectral / Fourier domain OCT ophthalmic imaging at 70,000 to 312,500 axial scans per second," Optics Express 16 (19), 15149-15169 (2008).

R. Huber, M. Wojtkowski, and J. G. Fujimoto, "Fourier Domain Mode Locking (FDML): A new laser operating regime and applications for optical coherence tomography," Optics Express 14(8), 3225-3237 (2006).

F. Fercher, C. K. Hitzenberger, G. Kamp, and S. Y. Elzaiat, "Measurement of Intraocular Distances by Backscattering Spectral Interferometry," Optics Communications, 117(1-2), 43-48 (1995).

S. R. Chinn, E. A. Swanson, and J. G. Fujimoto, "Optical coherence tomography using a frequency-tunable optical source," Optics Letters, 22(5), 340-342 (1997).

R. Leitgeb, C. K. Hitzenberger, and A. F. Fercher, "Performance of Fourier domain vs. time domain optical coherence tomography," Optics Express 11(8), 889-894 (2003).

J. F. de Boer, B. Cense, B. H. Park, M. C. Pierce, G. J. Tearney, and B. E. Bouma, "Improved signal-to-noise ratio in spectral-domain compared with time-domain optical coherence tomography," Optics Letters, 28 (21), 2067-2069 (2003).

M. A. Choma, M. V. Sarunic, C. H. Yang, and J. A. Izatt, "Sensitivity advantage of swept source and Fourier domain optical coherence tomography," Optics Express 11(18), 2183-2189 (2003).

V. Jayaraman, G.D. Cole, M. Robertson, A. Uddin and A. Cable, "High-sweep-rate 1310 nm MEMS-VCSEL with 150 nm continuous tuning range", Electronics Letters, vol. 48, No. 14, Jul. 5, 2012.

Marinko V. Sarunic, Brian E. Applegate, and Joseph A. Izatt, "Real-time quadrature projection complex conjugate resolved Fourier domain optical coherence Tomography", Optics Letters, vol. 31, No. 16, Aug. 15, 2006.

Youxin Mao, Costel Flueraru, Shoude Chang, Dan P. Popescu, Michael G. Sowa, "Performance analysis of a swept-source optical coherence tomography system with a quadrature interferometer and optical amplification", Optics Communications, vol. 284, Issues 10-11, May 15, 2011.

V. Duc Nguyen, N. Weiss, W. Beeker, M. Hoekman, A. Leinse, R. G. Heideman, T. G. van Leeuwen, and J. Kalkman, "Integrated-optics-based swept-source optical coherence tomography", Optics Letters, vol. 37, No. 23, Dec. 1, 2012.

B. Imran Akca, Markus Pollnau, Kerstin Worhoff, Rene M. De Ridder, "Silicon Oxynitride Technology for Integrated Optical Solutions in Biomedical Applications", In: 13th International Conference on Transparent Optical Networks 2011, Jun. 26-30, 2011, Stockholm, Sweden.

B. Imran Akca, "Spectral-Domain Optical Coherence Tomography on a Silicon Chip", PhD Thesis. University of Twente, (2012).

B. I. Akca, V. Nguyen, J. Kaulkman, N. Ismail, G. Sengo, Sen Fei, A. Dressen, T.G. Leeuwen, M. Pallnau, K. Sorhoff, R.M. De Ridder, "Toward Spectral-Domain Optical Coherence Tomography on a Chip", IEEE Journal of Quantum Electronics, vol. 18, Issue 3, 2012.

D. Culemann, A. Knuettel, and E. Voges, "Integrated optical sensor in glass for optical coherence tomography," IEEE J. Sel. Topics Quantum Electron., vol. 6, No. 5, pp. 730-734, Oct. 2000.

E. Margallo-Balbas,M. Geljon, G. Pandraud, and P. J. French, "Miniature 10 kHz thermo-optic delay line in silicon," Opt. Lett., vol. 35, No. 23, pp. 4027-4029, Dec. 2010.

G. Yurtsever, P. Dumon, W. Bogaerts, and R. Baets, "Integrated photonic circuit in silicon on insulator for Fourier domain optical coherence tomography," in Proc. SPIE, Opt. Coherence Tomography Coherence Domain Opt. Methods Biomed. XIV, vol. 7554, San Francisco, CA, 2010, pp. 1-5.

V. D. Nguyen, N. Ismail, F. Sun, K. W"orhoff, T. G. van Leeuwen, and J. Kalkman, "SiON integrated optics elliptic couplers for Fizeau-based optical coherence tomography," IEEE J. Lightw. Technol., vol. 28, No. 19, pp. 2836-2842, Sep. 2010.

V. D. Nguyen, B. I. Akca, K. W"orhoff, R. de Ridder, M. Pollnau, T. G. van Leeuwen, and J. Kalkman, "Spectral domain optical coherence tomography imaging with an integrated optics spectrometer," Opt. Lett., vol. 36, No. 7, pp. 1293-1295, Apr. 2011.

K. W"orhoff, C. G. H. Roeloffzen, R. M. de Ridder, A. Driessen, and P. V. Lambeck, "Design and application of compact and highly tolerant polarization-independent waveguides," IEEE J. Lightw. Technol., vol. 25, No. 5, pp. 1276-1282, May 2007.

Kyle Preston, Arthur Nitkowski, Nicolás Sherwood-Droz, Andrew Berkeley, Bradley S. Schmid, and Arsen R. Hajian, OCTANE: Optical Coherence Tomography Advanced Nanophotonic Engine, CLEO 2013 Technical Digest, Paper AW31.5, Jun. 9-14, 2013.

Arthur Nitkowski, Kyle Preston, Nicolás Sherwood-Droz, Andrew Berkeley, Bradford B. Behr, Bradley S. Schmidt, and Arsen R. Hajian, "Nano Spectrometer for Optical Coherence Tomography", Imaging and Applied Optics Conference, Paper AM1B.3, (2013).

Daniel Neill, Luke Stewart, Huiping Li, Tom Killin, Fan Chen, Steve Frisken, Glenn Baxter, Simon Poole, "Compact polarization diverse receiver for biomedical imaging Applications", SPIE Proceedings, vol. 7891, Jan. 22, 2011.

Jiefeng Xi, Li Huo, Jiasong Li and Xingde Li, "Generic real-time uniform K-space sampling method for high-speed swept-Source optical coherence tomography", Optics Express, vol. 18, No. 9, Apr. 26, 2010.

C. M. Eigenwillig, B. R. Biedermann, G. Palte, and R. Huber, "K-space linear Fourier domain mode locked laser and applications for optical coherence tomography," Optics Express 16(12), 8916-8937 (2008).

R. Nagarajan et al., "10 channel, 100Gbit/s per channel, dual polarization, coherent QPSK, monolithic InP receiver photonic integrated circuit," Optical Fiber Communication Conference Proceeding, p. OML7. 2011.

M. Izutsu, S. Shikama, and T. Sueta, "Integrated optical SSB modulator/frequency shifter," IEEE J. Quant. Electron., vol. 2, No. 11, pp. 2225-2227, 1981.

D. Taillert, H. Chong, P. I. Borel, L. H. Frandsen, R. M. D. L. Rue, and R. Baets, "A compact two-dimensional grating coupler used as a polarization splitter", IEEE Photon. Tech. Lett., vol. 15, pp. 1249-1251, 2003.

(56) **References Cited**

OTHER PUBLICATIONS

N. Dupuis, C. R. Doerr, L. Zhang, L. Chen, N. J. Sauer, P. Dong, L. L. Buhl, and D. Ahn, "InP-based comb generator for optical OFDM," J. Lightw. Technol., 2011.

S. Chandrasekhar and Xiang Liu, "Enabling Components for Future High-Speed Coherent Communication Systems", Optical Fiber Communication Conference Tutorial, 2011.

G. Roelkens, D. Vermeulen, S. Selvaraja, Student Member, IEEE, R. Halir, W. Bogaerts, Member, IEEE, and D. Van Thourhout, "Grating-Based Optical Fiber Interfaces for Silicon-on-Insulator Photonic Integrated Circuits", IEEE Journal of Selected Topics in Quantum Electronics, vol. 17, No. 3, May/Jun. 2011.

Attila Mekis, Steffen Gloeckner, Gianlorenzo Masini, Adithyaram Narasimha, Member, IEEE, Thierry Pinguet, Subal Sahni, and Peter De Dobbelaere,"A Grating-Coupler-Enabled CMOS Photonics Platform". IEEE Journal of Selected Topics in Quantum Electronics, vol. 17, Issue 3, May/Jun. 2011.

Neil Na, Harel Frish, I-Wei Hsieh, Oshrit Harel, Roshan George, Assia Barkai, and Haisheng Rong, "Efficient broadband silicon-on-insulator grating coupler with low backreflection", Optics Letters, vol. 36, No. 11, Jun. 1, 2011.

Wissem Sfar Zaoui, Maria Félix Rosa, Wolfgang Vogel, Manfred Berroth Jörg Butschke, and Florian Letzkus, "Cost-effective CMOS-compatible grating couplers with backside metal mirror and 69% coupling efficiency", Optics Express, vol. 20, No. 26, Dec. 10, 2012.

Vilson R. Almeida, Roberto R. Panepucci, and Michal Lipson, "Nanotaper for compact mode conversion", Optics Letters, vol. 28, No. 15, Aug. 1, 2003.

Anatol Khilo, Miloš A. Popović, Mohammad Araghchini, and Franz X. Kärtner, "Efficient planar fiber-to-chip coupler based on two stage adiabatic evolution", Optics Express, vol. 18, No. 15, Jul. 19, 2010.

Long Chen, Member, IEEE, Christopher R. Doerr, Fellow, IEEE, Young-Kai Chen, Fellow, IEEE, and Tsung-Yang Liow, "Low-Loss and Broadband Cantilever Couplers Between Standard Cleaved Fibers and High-Index-Contrast Si3N4 or Si Waveguides", IEEE Photonics Technology Letters, vol. 22, No. 23, Dec. 1, 2010.

Alan Y. Liu, Chong Zhang, Justin Norman, Andrew Snyder, Dmitri Lubyshev,Joel M. Fastenau, Amy W. K. Liu, Arthur C. Gossard, and John E. Bowers, "High performance continuous wave 1.3 Im quantum dot lasers on silicon", Applied Physics Letters 104, 041104 (2014).

B. I. Akca, B. Povazay, A. Alex, K. Worhoff, R. M. de Ridder, W. Drexler, and M. Pallnau, "Miniature spectrometer and beam splitter for an optical coherence tomography on a silicon chip", Optics Express, vol. 31, No. 14, Jul. 3, 2014.

Günay Yurtsever, Boris Považay, Aneesh Alex, Behrooz Zabihian, Wolfgang Drexler, and Roel Baets, "Photonic integrated Mach-Zehnder interferometer with an on-chip reference arm for optical coherence tomography", Optics Express, vol. 5, No. 4, Mar. 3, 2014.

Haitham Omran, Yasser M. Sabry, Mohamed Sadek, Khaled Hassan, Mohamed Y. Shalaby and Diaa Khalil, "Deeply-Etched Optical MEMS Tunable Filter for Swept Laser Source Applications", IEEE Photonics Technology Letters. vol. 26, No. 1, Jan. 2014.

V. Jayaraman, G.D. Cole, M. Robertson, C. Burgner, D. John, A. Uddin and A. Cable, "Rapidly swept, ultra-widely-tunable 1060 nm MEMS-VCSELs", Electronics Letters, Oct. 11, 2012 vol. 48 No. 21.

Aflatouni et al., Nanophotonic coherent imager. Opt Express. Feb. 23, 2015;23(4):5117-25. doi:10.1364/OE.23.005117.

Biedermann et al., Dispersion, coherence and noise of Fourier domain mode locked lasers. Opt Express. Jun. 8, 2009;17(12):9947-61.

Blatter et al., High-speed functional OCT with self-reconstructive Bessel illumination at 1300 nm. Proc SPIE 8091, Optical Coherence Tomography and Coherence Techniques V. Jun. 1, 2011;809104.1-6. Doi:10.1117/12.889669.

Brzobohatý et al., High quality quasi-Bessel beam generated by round-tip axicon. Opt Express. Aug. 18, 2008;16(17):12688-700.

Burns et al., A Wafer-Scale 3-D Circuit Integration Technology. IEEE Trans Electronic Devices. Oct. 2006;53(10):2507-16.

Chen et al., Monolithically integrated 40-wavelength demultiplexer and photodetector array on silicon. IEEE Photon Technol Lett. Jun. 6, 2011;23(13):869-71.

Choi et al., Phase-sensitive swept-source optical coherence tomography imaging of the human retina with a vertical cavity surface-emitting laser light source. Opt Lett. Feb. 1, 2013;38(3):338-40. Epub Jul. 24, 2013. 7 pages.

De Boer et al., Review of polarization sensitive optical coherence tomography and Stokes vector determination. J Biomed Opt. Jul. 2002;7(3):359-71.

Derose et al., Electronically controlled optical beam-steering by an active phased array of metallic nanoantennas. Opt Express. Feb. 25, 2013;21(4):5198-208.

Doerr et al., Single-chip silicon photonics 100-Gb/s coherent transceiver. Optical Fiber Communication Conference: Postdeadline Papers, (Optical Society of America, 2014), Paper Th5C.1. San Francisco, CA. Mar. 9-13, 2014;1-3.

Doylend et al., Two-dimensional free-space beam steering with an optical phased array of silicon-on-insulator. Opt Express. Oct. 24, 2011;19(22):21595-604.

Drexler et al., Optical Coherence Tomography: Technology and Applications. 2nd ed. Springer International Publishing, Switzerland. 2015. Cover page and table of contents only. 9 pages.

Gourley et al., First experimental demonstration of a Fresnel Axicon. Proc. SPIE 7099, Photonics North. Aug. 11, 2008;7099:70990D.1-7. Doi:10.1117/12.807162.

Hee et al., Polarization-sensitive low-coherence reflectometer for birefringence characterization and ranging. J Opt Soc Am B. Jun. 1992;9(6):903-8.

Hofer et al., Dispersion encoded full range frequency domain optical coherence tomography. Opt Express. Jan. 5, 2009;17(1):7-24.

Huber et al., Buffered Fourier domain mode locking: unidirectional swept laser sources for optical coherence tomography imaging at 370,000 lines/s. Opt Lett. Oct. 15, 2006;31(20):2975-7.

Jia et al., Split-spectrum amplitude-decorrelation angiography with optical coherence tomography. Opt Express. Feb. 13, 2012;20(4):4710-25.

Lee et al., Dual detection full range frequency domain optical coherence tomography. Opt Lett. Apr. 1, 2010;35(7):1058-60.

Leon-Saval et al., Mode-selective photonic lanterns for space division multiplexing. Opt Express. Jan. 13, 2014;22(1):1-9.

Lorenser et al., Energy-efficient low-Fresnel-number Bessel beams and their application in optical coherence tomography. Opt Lett. Feb. 1, 2014;39(3):548-51.

Lu et al., Handheld ultrahigh speed swept source optical coherence tomography instrument using a MEMs scanning mirror. Biomed Opt Express. Jan. 1, 2014;5(1):293-311.

Makita et al., Optical coherence angiography. Opt Express. Aug. 21, 2006;14(17):7821-40.

Margallo-Balbás et al., Miniature Optical Coherence Tomography System Based on Silicon Photonics. Proc SPIE 6847, Coherence Domain Optical Methods and Optical Coherence Tomography in Biomedicine XII. Feb. 28, 2008;6857:684705.1-11.

Mekis et al., Two-dimensional photonic crystal couplers for unidirectional light output. Opt Lett. Jul. 1, 2000;25(13):942-4.

Merola et al., Fabrication and test of polymeric microaxicons. Proc SPIE 8428, Micro-Optics 2012. Jun. 1, 2012;8428:84280P.1-11. Doi:10.1117/12.922572.

Morgner et al., Spectroscopic optical coherence tomography. Opt Lett. Jan. 15, 2000;25(2):1113.

Nadkarni et al., Measurement of Collagen and Smooth Muscle Cell Content in Atherosclerotic Plaques Using Polarization-Sensitive Optical Coherence Tomography. J Am Coll Cardiol. Apr. 3, 2007;49(13):1474-81. Epub Nov. 30, 2009. 15 pages.

Pahlevaninezhad et al., Fiber-Based Polarization Diversity Detection for Polarization-Sensitive Optical Coherence Tomography. Photon. Sep. 30, 2014;1(4):283-95.

(56) **References Cited**

OTHER PUBLICATIONS

Park et al., III-V/SOI Vertical Cavity Laser with In-plane Output into a Si Waveguide. Optical Fiber Communications Conference and Exhibition (OFC), 2015, Los Angeles, CA. Mar. 22-26, 2015. Paper W2A.17. 2 pages.

Park et al., Hybrid III-V/SOI single-mode vertical-cavity laser with in-plane emission into a silicon waveguide. 2015 Conference on Lasers and Electro-Optics. San Jose, CA. May 10-15, 2015. Paper SW3F.2. 2 pages.

Park et al., Jones matrix analysis for a polarization-sensitive optical coherencetomography system using fiber-optic components. Opt Lett. Nov. 1, 2004;29(21):2512-4. Epub Jun. 9, 2009. 7 pages.

Pircher et al., Polarization sensitive optical coherence tomography in the human eye. Prog Retin Eye Res. 2011;30(6):431-51. Doi: 10.1016/j.preteyeres.2011.06.003.

Potsaid et al., MEMS tunable VCSEL light source for ultrahigh speed 60kHz-1MHz axial scan rate and long range centimeter class OCT imaging. Proc SPIE 8213, Optical Coherence Tomography and Coherence Domain Optical Methods in Biomedicine XVI, 82130M. Feb. 9, 2012. Doi:10.1117/12.911098. 5 pages.

Ralston et al., Interferometric synthetic aperture microscopy. Nat Phys. Jan. 21, 2007;3(2):12934. 6 pages.

Ryf et al., Photonic-Lantern-Based Mode Multiplexers for Few-Mode-Fiber Transmission. Optical Fiber Communications Conference and Exhibition (OFC), 2014. San Francisco, CA. Paper W4J.2. Mar. 9-13, 2014;1-3.

Sarunic et al., Instantaneous complex conjugate resolved spectral domain and swept-source OCT using 3×3 fiber couplers. Opt Express. Feb. 7, 2005;13(3):957-67.

Schneider et al., Optical coherence tomography system mass-producible on a silicon photonic chip. Opt Express. Jan. 20, 2016;24(2):1573-86.

Selvaraja et al., Record low-loss hybrid rib/wire waveguides for silicon photonic circuits. 7th International Conference on Group IV Photonics, Beijing, China. Sep. 1-3, 2010. 3 pages.

Siddiqui et al., Compensation of spectral and RF errors in swept-source OCT for high extinction complex demodulation. Opt Express. Mar. 9, 2015;23:5508-20.

Sokolovskii et al., Bessel beams from semiconductor light sources. Prog Quantum Electron. Jul. 2014;38(4):157-88.

Steinvurzel et al., Fiber-based Bessel beams with controllable diffraction-resistant distance. Opt Lett. 2011;36(23):4671-3.

Stutzman et al., Antenna Theory and Design. John Wiley & Sons, New York. 1981. Cover page and table of contents only. 8 pages.

Sun et al., Large-scale nanophotonic phased array. Nature. Jan. 10, 2013;493:195-9.

Sun et al., Large-Scale Silicon Photonic Circuits for Optical Phased Arrays. IEEE J Selected Topics Quantum Electron. Jul./Aug. 2014;20(4). 15 pages.

Sun et al., Two-dimensional apodized silicon photonic phased arrays. Opt Lett. Jan. 15, 2014;39(2):367-70.

Tearney et al., Spectrally Encoded Confocal Microscopy. Opt Lett. Aug. 1, 1998;23(15):1152-4.

Tsai et al., Ultrahigh speed endoscopic optical coherence tomography using micromotor imaging catheter and VCSEL technology. Biomed Opt Express. Jun. 14, 2013;4(7):1119-32.

Vakoc et al., Elimination of depth degeneracy in optical frequency-domain imaging through polarization-based optical demodulation. Opt Lett. Feb. 1, 2006;31(3):362-4. Epub Jul. 20, 2009. 8 pages.

Vakoc et al., Phase-resolved optical frequency domain imaging. Opt Express. Jul. 11, 2005;13(14):5483-93.

Van Acoleyen et al., Two-dimensional optical phased array antenna on silicon-on-insulator. Opt Express. Jun. 21, 2010;18(13):13655-60.

Vermeulen et al., High-efficiency fiber-to-chip grating couplers realized using an advanced CMOS-compatible silicon-on-insulator platform. Opt Express. Aug. 16, 2010;18(17):18278-83.

Vermeulen et al., Silicon-on-insulator polarization rotator based on a symmetry breaking silicon overlay. IEEE Photon Technol Lett. Mar. 15, 2012;24(5):482-4.

Wang et al., Depth-encoded all-fiber swept source polarization sensitive OCT. Biomed Opt Express. Sep. 1, 2014;5(9):2931-49.

Wang et al., Three dimensional optical angiography. Opt Express. Apr. 2, 2007;15(7):4083-97.

Wang, In vivo full range complex Fourier domain optical coherence tomography. Appl Phys Lett. Jan. 30, 2007;90(5):054103.1-3.

Weber et al., Highly compact imaging using Bessel beams generated by ultraminiaturized multi-micro-axicon systems. J Opt Soc Amer A. May 2012; 29(5):808-16.

Wieser et al., High definition live 3D-OCT in vivo: design and evaluation of a 4D OCT engine with 1 GVoxel/s. Biomed Opt Express. Sep. 1, 2014;5(9):2963-77.

Wojtkowski et al., Full range complex spectral optical coherence tomography technique in eye imaging. Opt Lett. 2002;27(16):1415-7.

Wörhoff et al., Silicon Oxynitride Technology for Integrated Optical Solutions in Biomedical Applications. 2011 13th International Conference on Tranparent Optical Networks. Stockholm, Sweden. Jun. 26-30, 2011. 4 pages.

Xie et al., Axicon on a gradient index lens (AXIGRIN)): integrated otial bench for Bessel beam generation from a point-like source. Appl Opt. 2014;53(26):6103-7.

Yaacobi et al., Vertical emitting aperture nanoantennas. Opt Lett. May 1, 2012;37(9):1454-6.

Yamanari et al., Full-range polarization-sensitive swept-source optical coherence tomography by simultaneous transversal and spectral modulation. Opt Express. 2010;18(13):13964-80.

Yazdanfar et al., High resolution imaging of in vivo cardiac dynamics using color Doppler optical coherence tomography. Opt Express. Dec. 22, 1997;1(13):424-31.

Yun et al., High-speed optical frequency-domain imaging. Opt Express. Nov. 3, 2003;11(22):295363.

Yun et al., Removing the depth-degeneracy in optical frequency domain imaging with frequency shifting. Opt Express. Oct. 4, 2004;12(20):4822-8.

Yurtsever et al., Ultra-compact silicon photonic integrated interferometer for swept-source optical coherence tomography. Opt Lett. Sep. 1, 2014;39(17):5228-31.

Zhao et al., Phase-resolved optical coherence tomography and optical Doppler tomography for imaging blood flow in human skin with fast scanning speed and high velocity sensitivity. Opt. Lett. Jan. 15, 2000;25(2):114-6.

* cited by examiner

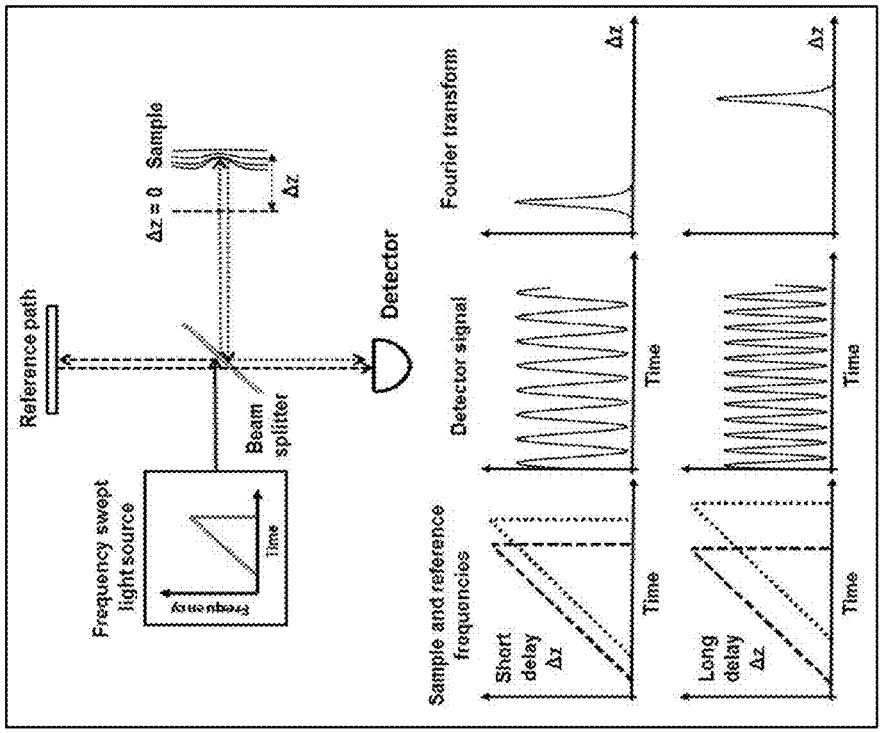
Reference path
Frequency swept light source
Frequency
Time
Beam splitter
Δz = 0
Sample
Δz
Detector
Fourier transform
Detector signal
Sample and reference frequencies
Short delay Δz
Long delay Δz
Time
Δz

FIGURE 1(a)

Example Specifications

- Center Wavelength ~ 1310 nm
- Scan Range > 100 nm
- Coherence Length > 20 mm
- Sweep Speed > 100 kHz
- Laser Output Power > 25 mW
- Ideal sweep 100% duty cycle sawtooth

FIGURE 1(b)

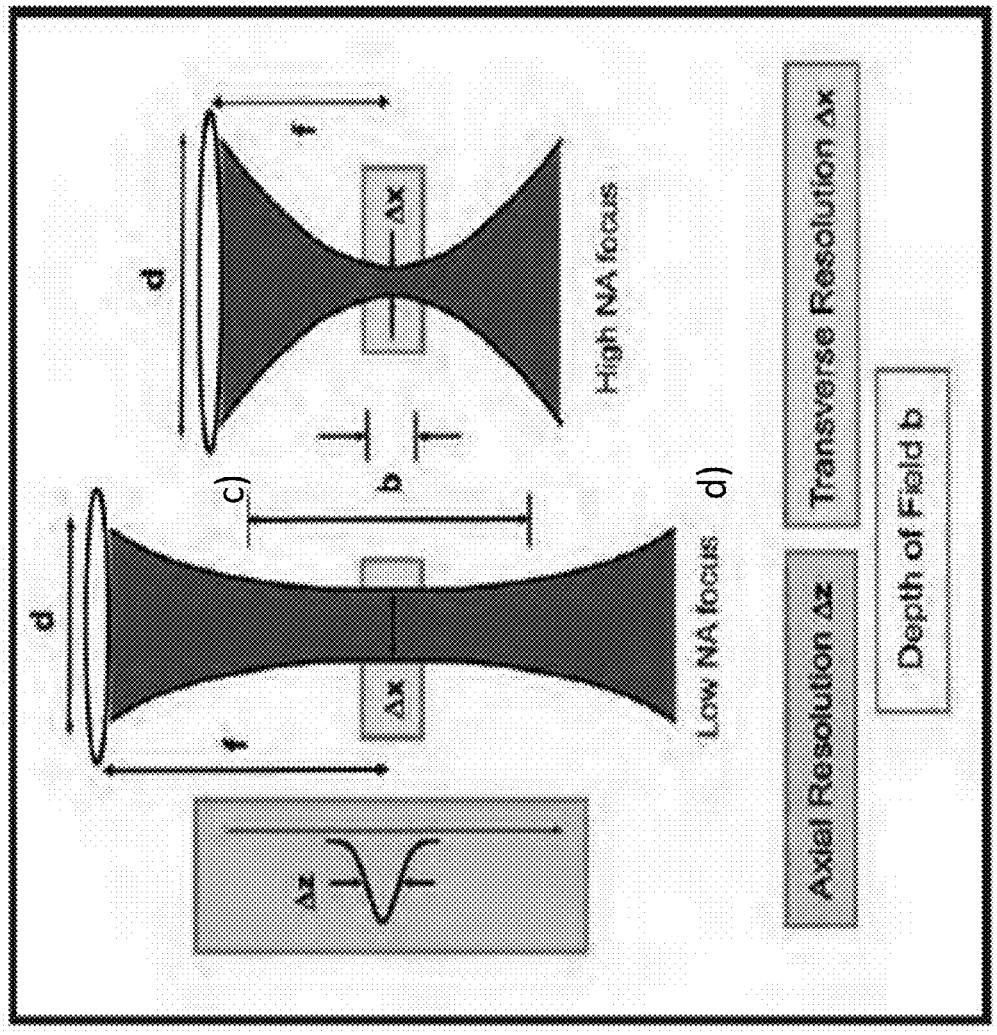
d
f
Δx
High NA focus
c)
b
d)
Low NA focus
Δz
Axial Resolution Δz
Transverse Resolution Δx
Depth of Field b

Figure 1(c)

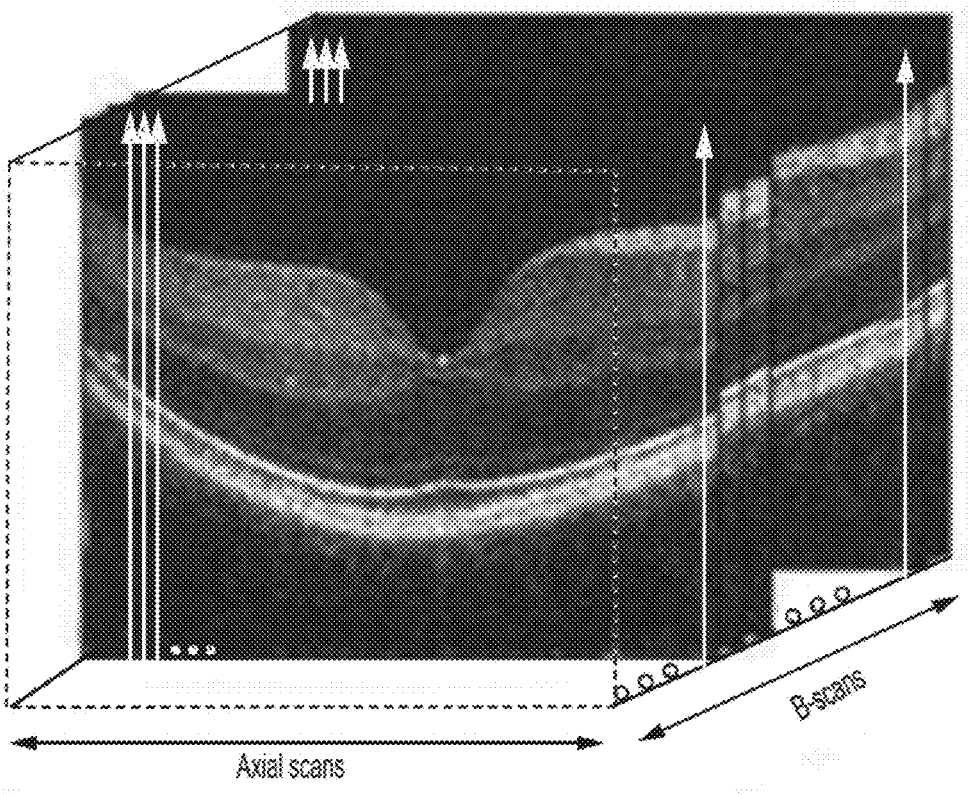

FIGURE 1(d)

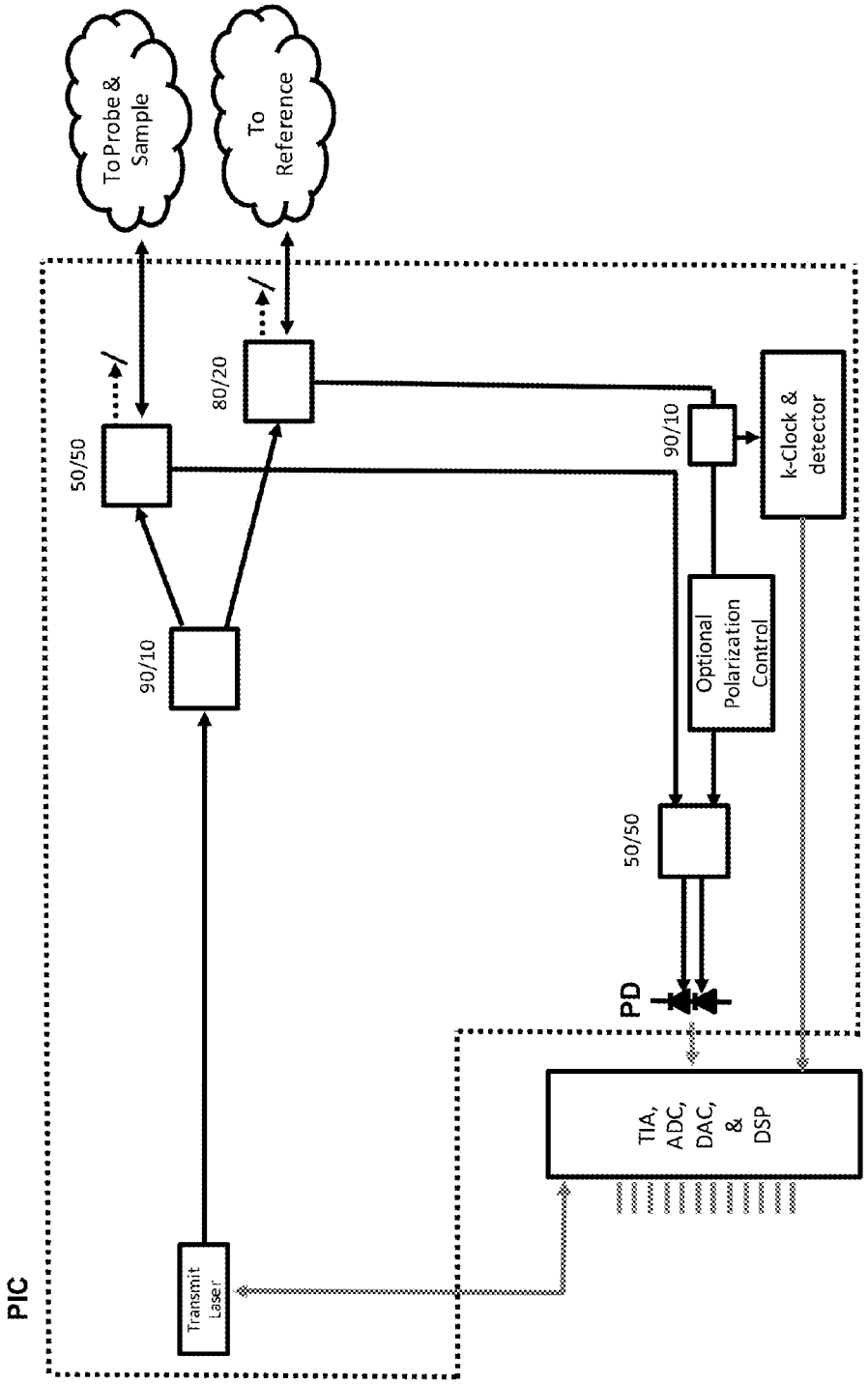
To Probe & Sample
To Reference
80/20
50/50
90/10
90/10
k-Clock & detector
Optional Polarization Control
50/50
PD
TIA, ADC, DAC, & DSP
Transmit Laser
PIC

FIGURE 2

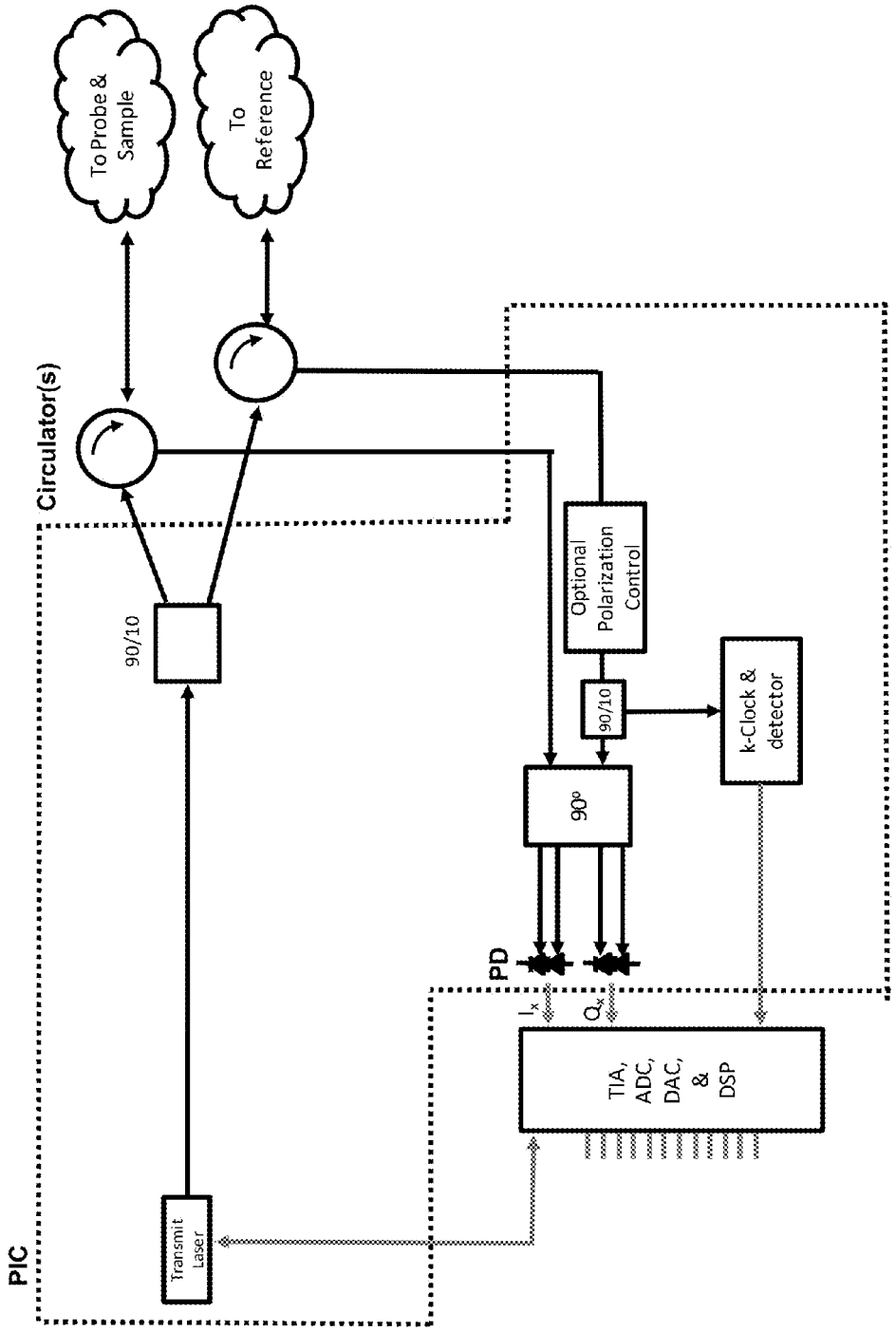
To Probe & Sample
To Reference
Circulator(s)
90/10
Optional Polarization Control
90/10
k-Clock & detector
90°
PD
I_x
Q_x
TIA, ADC, DAC, & DSP
Transmit Laser
PIC

FIGURE 3

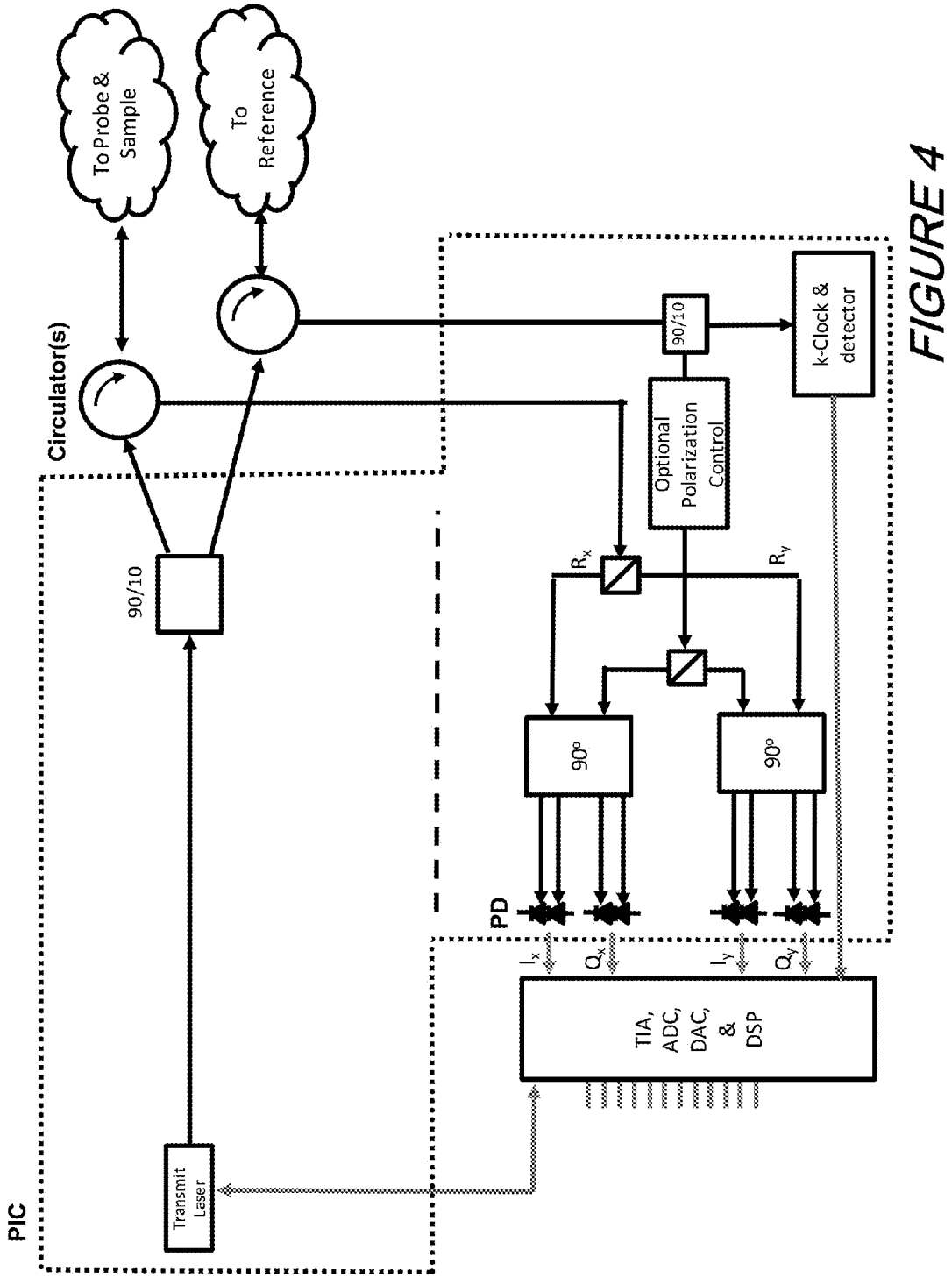
To Probe & Sample
To Reference
Circulator(s)
90/10
90/10
k-Clock & detector
Optional Polarization Control
R_x
R_y
90°
90°
PD
I_x
Q_x
I_y
Q_y
TIA, ADC, DAC, & DSP
Transmit Laser
PIC

FIGURE 4

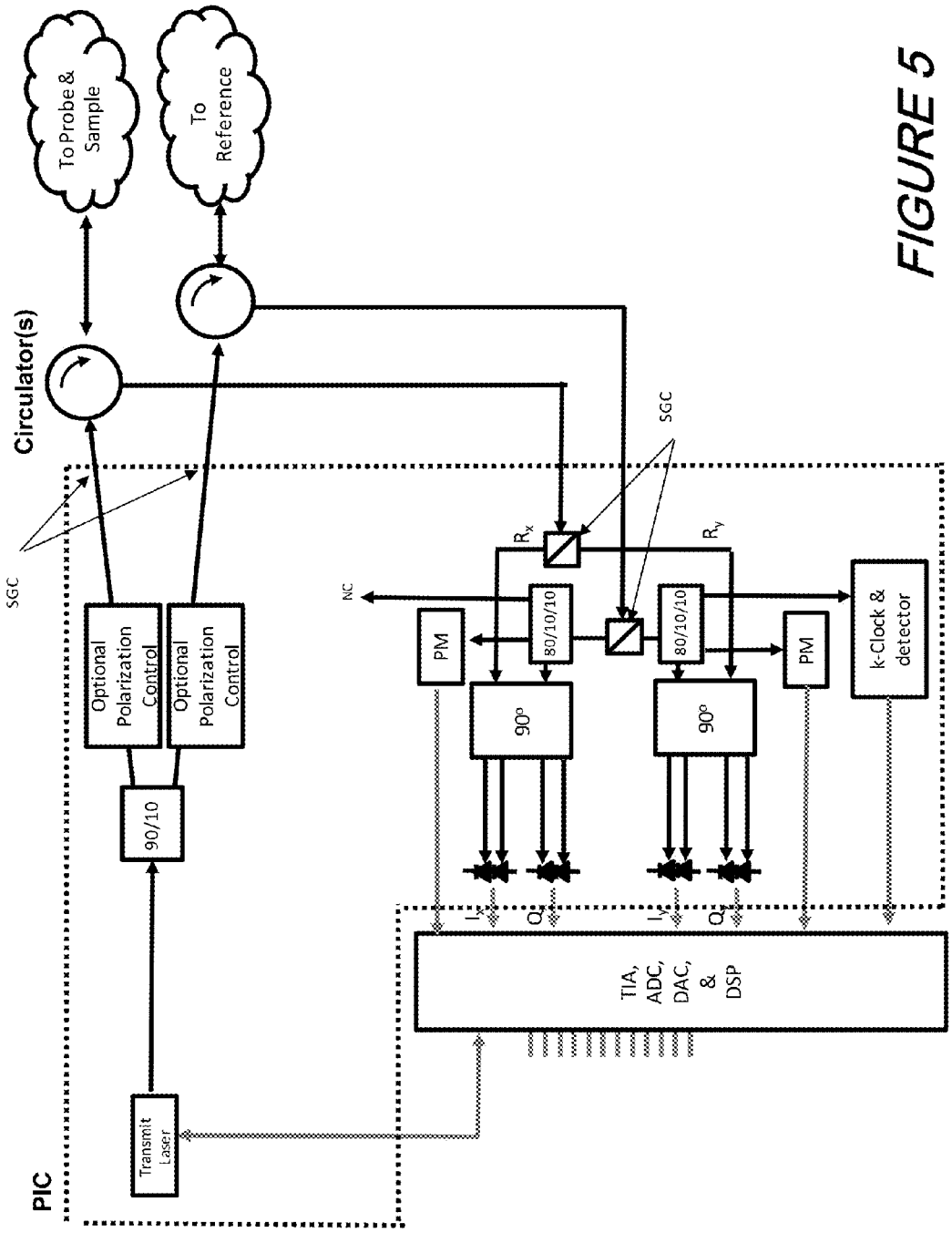
To Probe & Sample
To Reference
Circulator(s)
SGC
SGC
Optional Polarization Control
Optional Polarization Control
90/10
Transmit Laser
PIC
NC
PM
80/10/10
80/10/10
PM
k-Clock & detector
90°
90°
TIA, ADC, DAC, & DSP

FIGURE 5

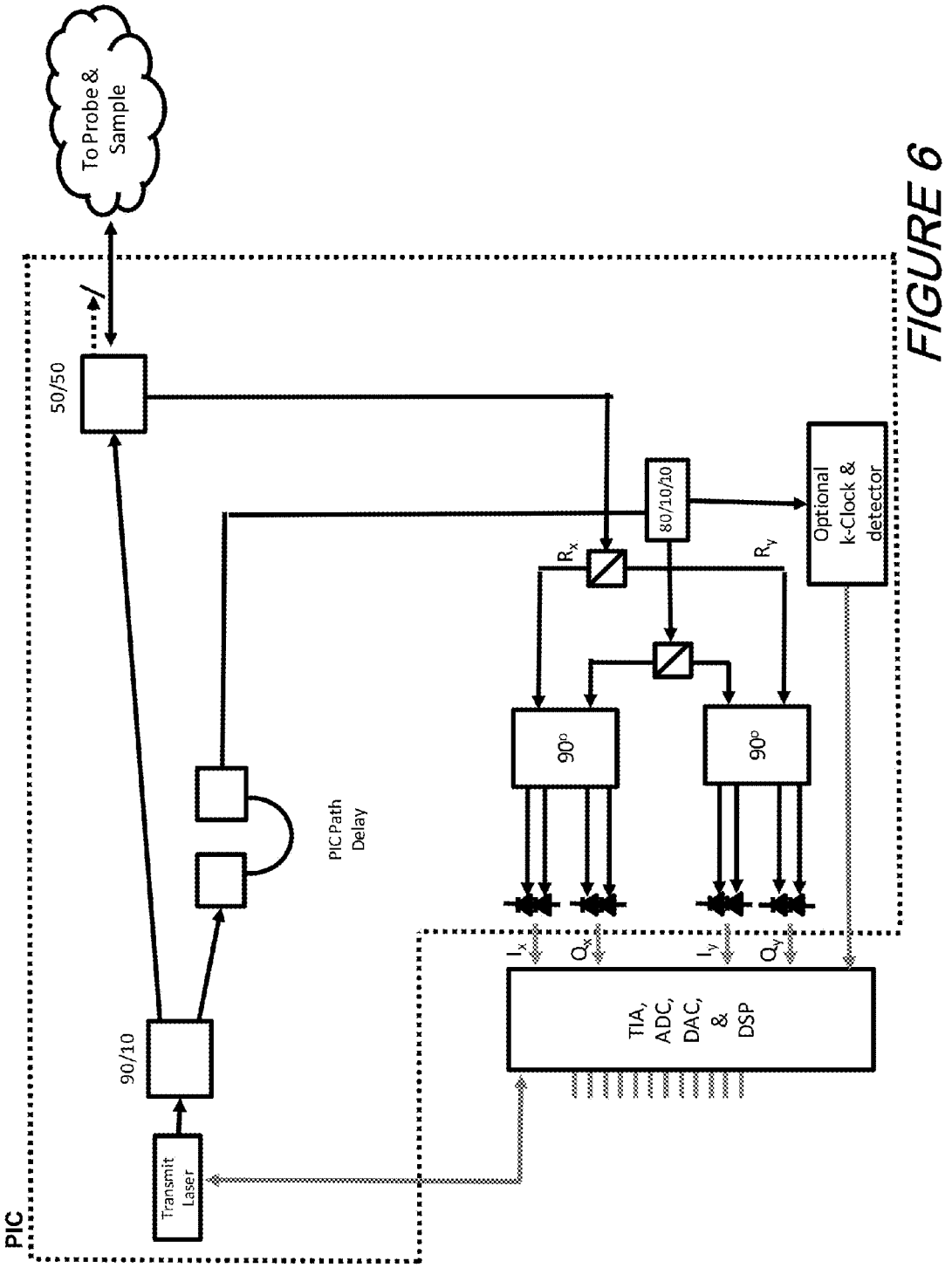
To Probe & Sample
50/50
80/10/20
Optional k-Clock & detector
R_x
R_y
90°
90°
PIC Path Delay
90/10
Transmit Laser
PIC
I_x
Q_x
I_y
Q_y
TIA, ADC, DAC, & DSP

FIGURE 6

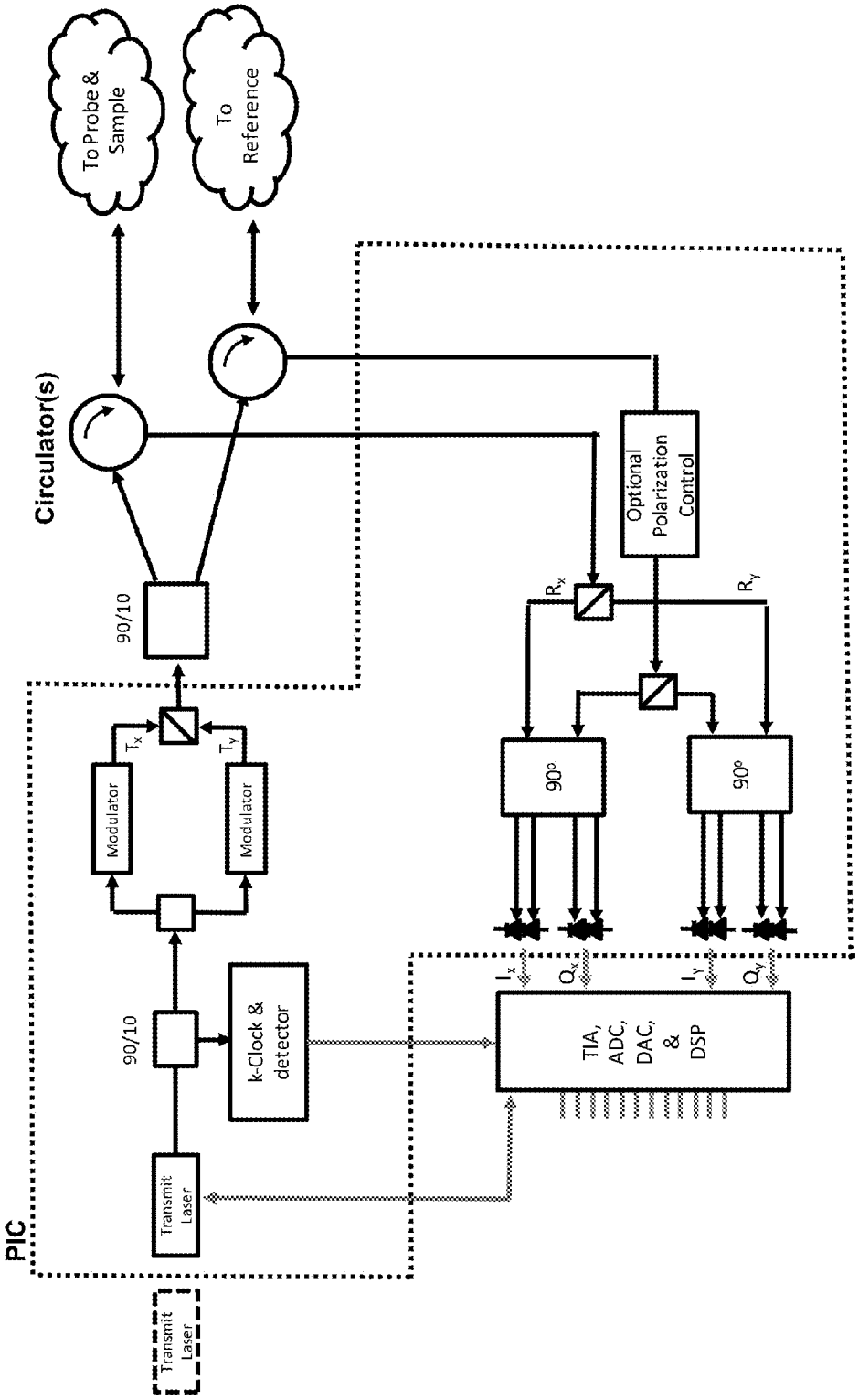
To Probe & Sample
To Reference
Circulator(s)
90/10
Optional Polarization Control
R_x
R_y
90°
90°
T_x
T_y
Modulator
Modulator
90/10
k-Clock & detector
I_x
Q_x
I_y
Q_y
TIA, ADC, DAC, & DSP
Transmit Laser
PIC
Transmit Laser

FIGURE 7

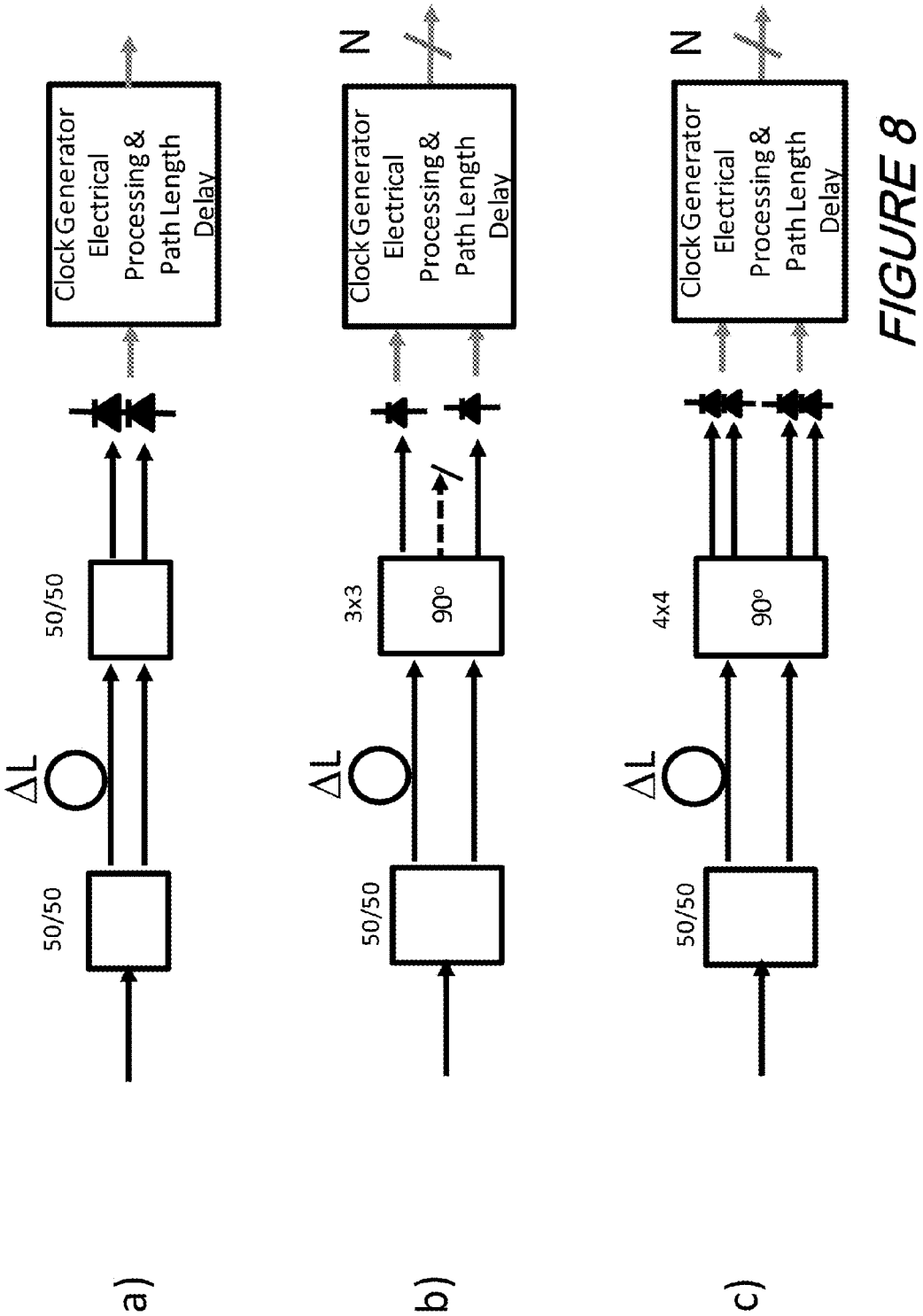
Clock Generator
Electrical
Processing &
Path Length
Delay
50/50
ΔL
50/50
a)
N
3x3
90°
b)
4x4
c)

FIGURE 8

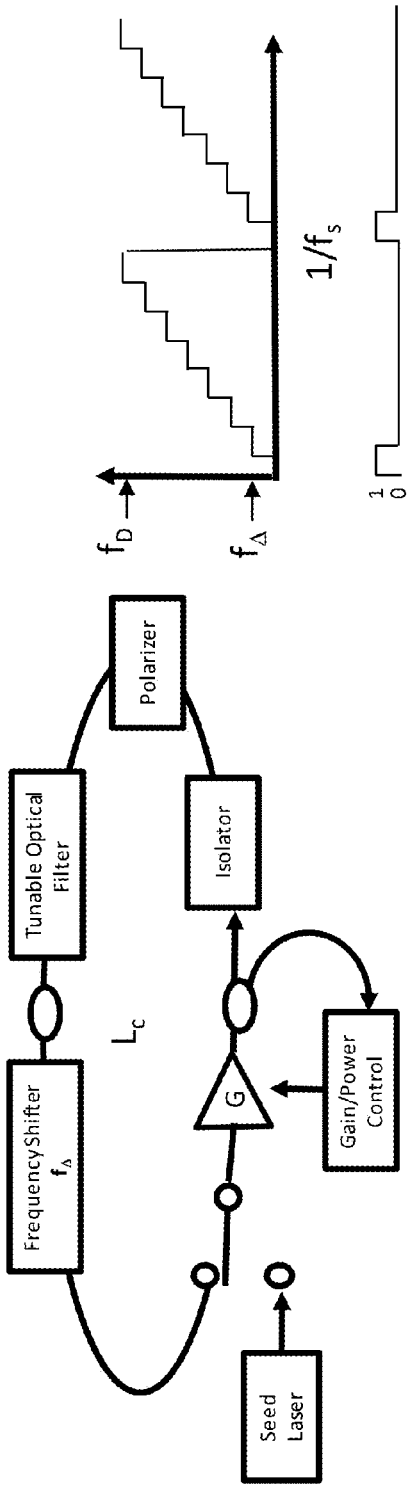
Polarizer
Tunable Optical Filter
Isolator
L_C
Frequency Shifter f_Δ
G
Gain/Power Control
Seed Laser
f_D
f_Δ
$1/f_s$
1
0

FIGURE 9(a)

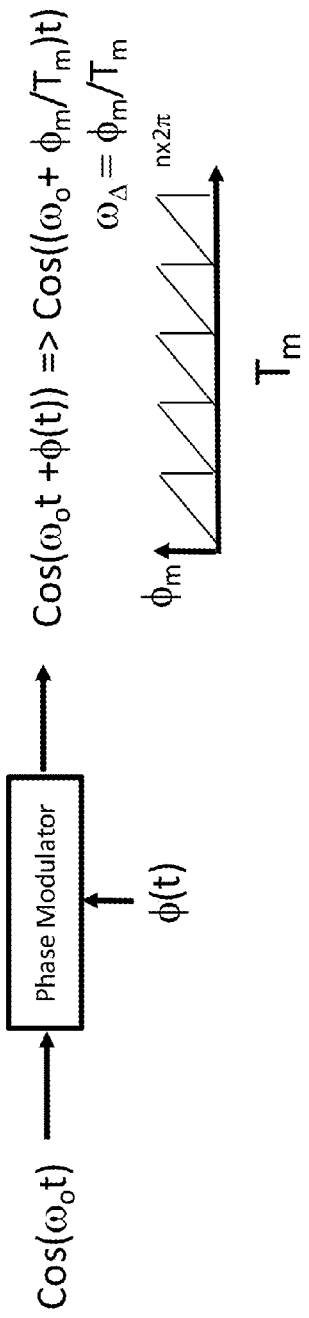
Cos(ωot)
Phase Modulator
ϕ(t)
Cos(ωot +ϕ(t)) => Cos((ωo+ ϕm/Tm)t)
ωΔ = ϕm/Tm
nx2π
ϕm
Tm

FIGURE 9(b)

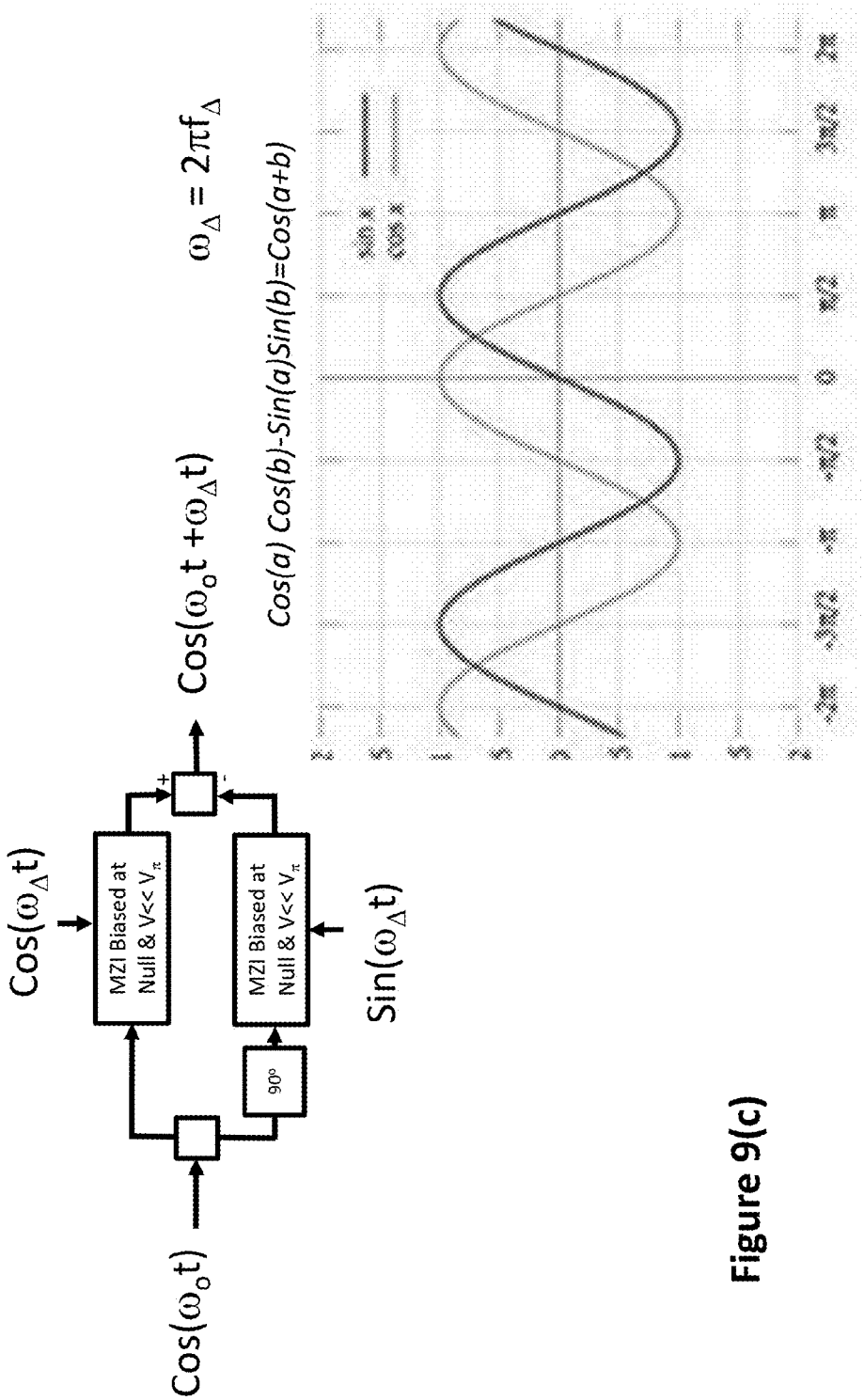
$\omega_\Delta = 2\pi f_\Delta$
$Cos(\omega_o t + \omega_\Delta t)$
$Cos(a)\ Cos(b)-Sin(a)Sin(b)=Cos(a+b)$
$Cos(\omega_\Delta t)$
MZI Biased at Null & V<< V_π
MZI Biased at Null & V<< V_π
90°
$Sin(\omega_\Delta t)$
$Cos(\omega_o t)$

Figure 9(c)

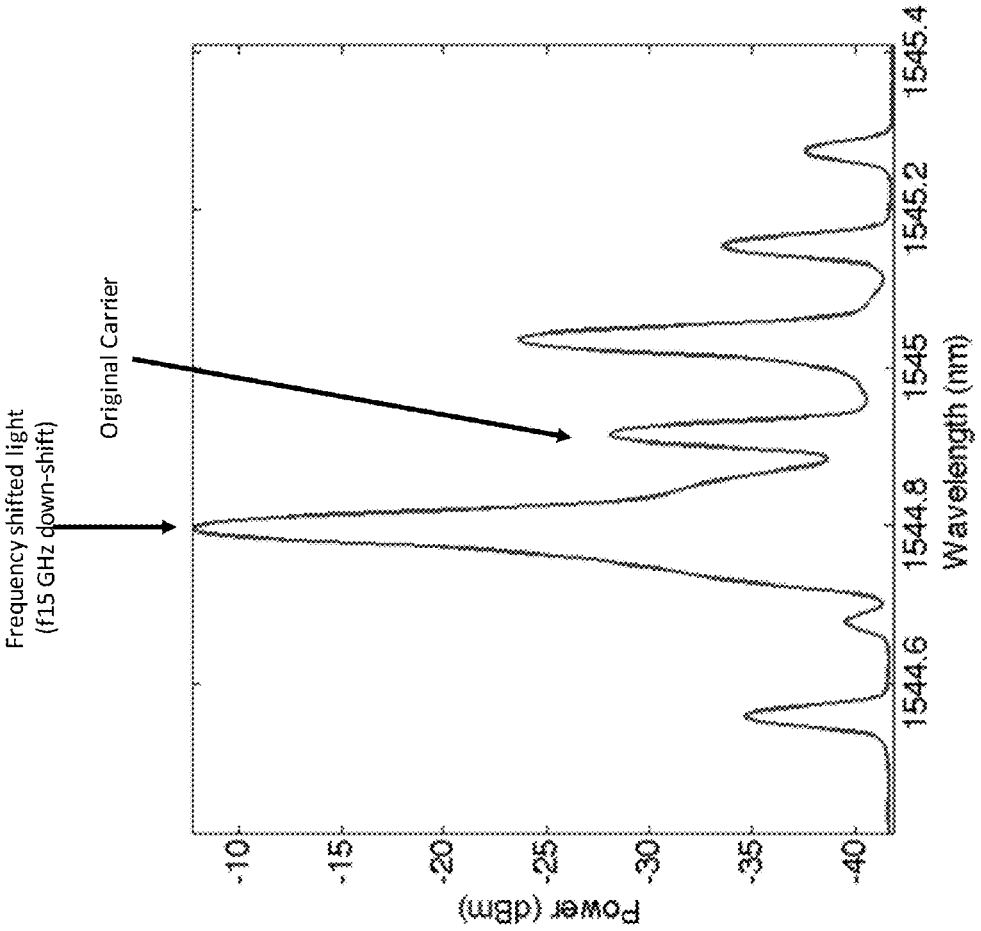
Frequency shifted light
(f15 GHz down-shift)
Original Carrier
Power (dBm)
-10
-15
-20
-25
-30
-35
-40
1544.6
1544.8
1545
1545.2
1545.4
Wavelength (nm)

FIGURE 10

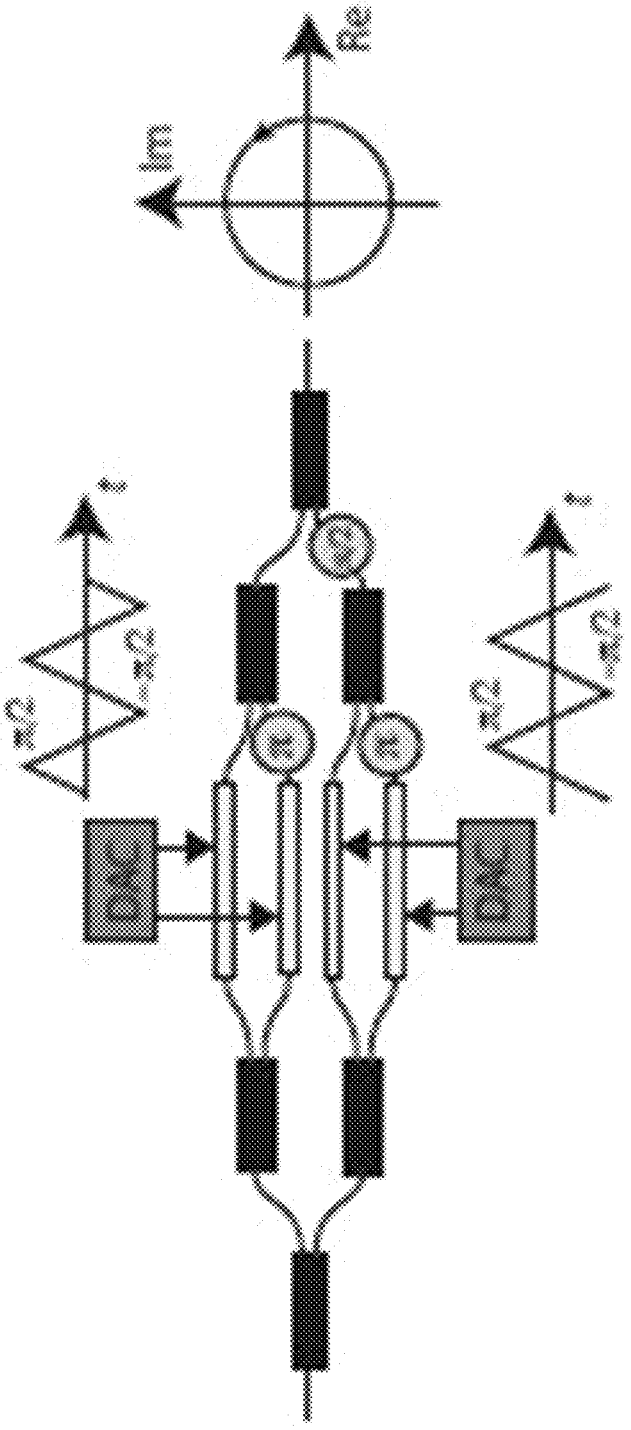

Figure 11(a)

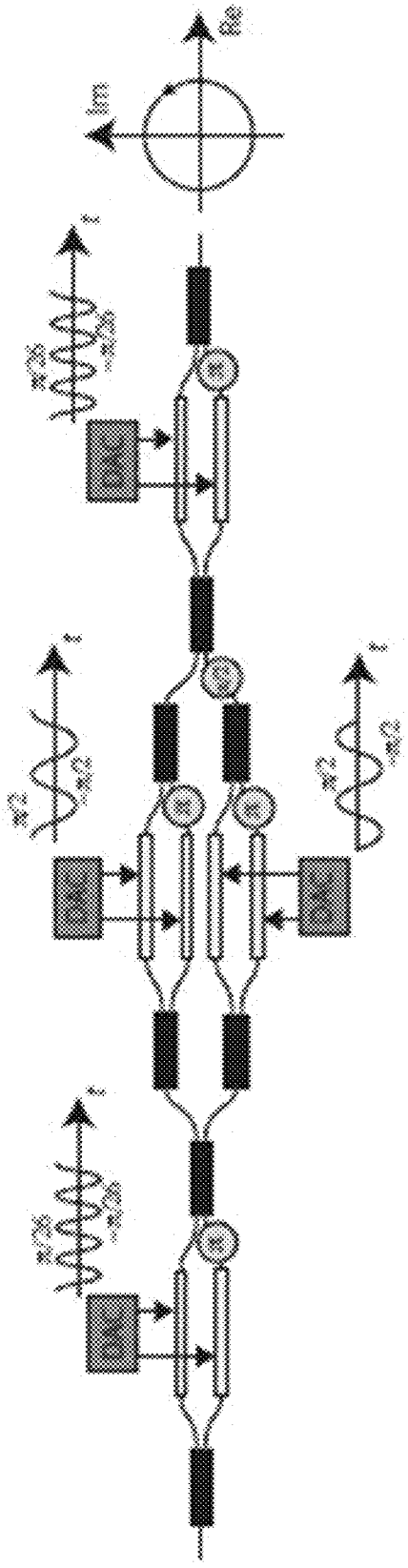

Figure 11(b)

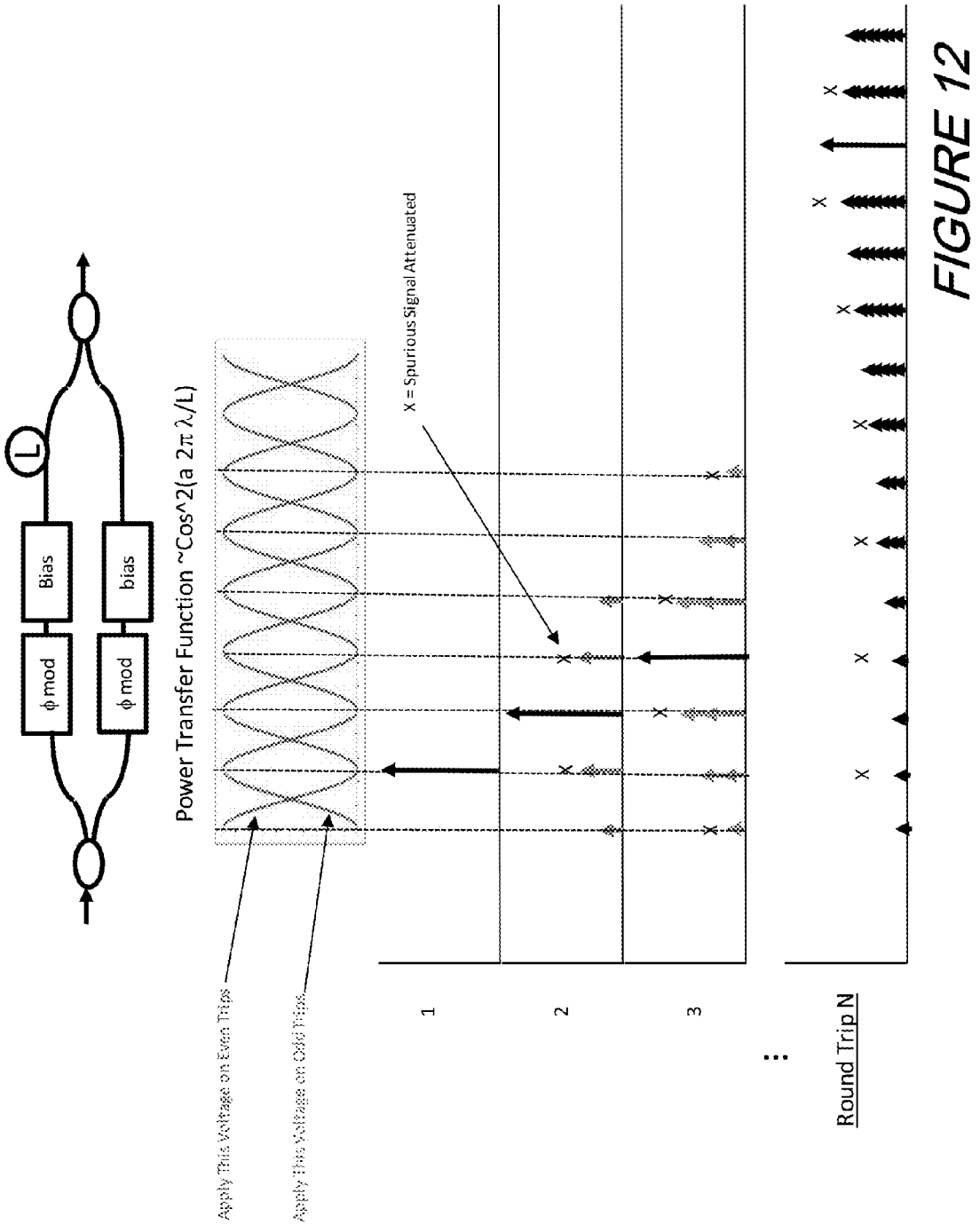
L
Bias
bias
ϕ mod
ϕ mod
Power Transfer Function ~Cos^2(a 2π λ/L)
X = Spurious Signal Attenuated
Apply This Voltage on Even Trips
Apply This Voltage on Odd Trips
1
2
3
...
Round Trip N

FIGURE 12

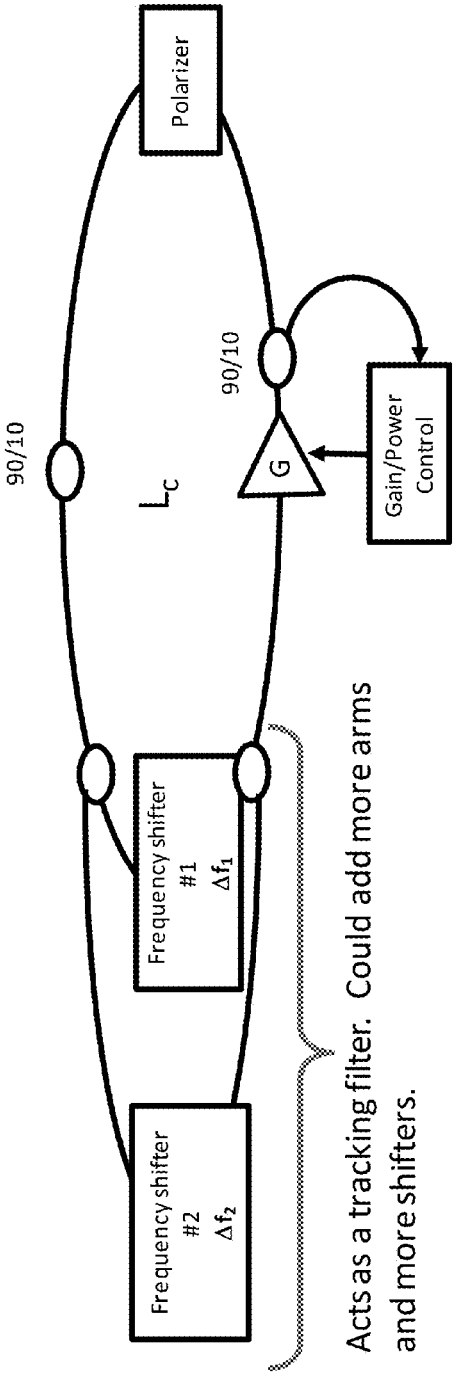

$\Delta f_2 \sim \Delta f_1(1+\Delta L/Lc)$, where ΔL ~ MZI path length difference and Lc ~ cavity length

FIGURE 13

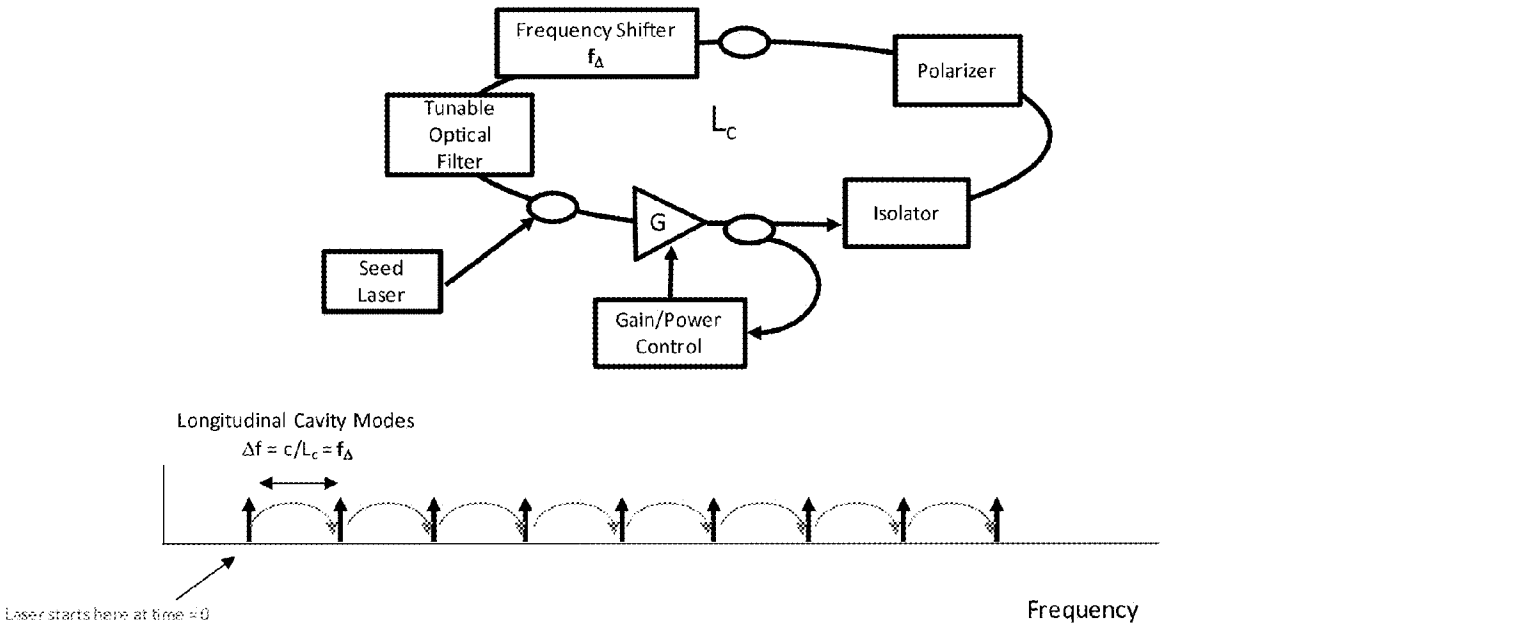

Example Parameters

λ_o= Center Wavelength ~ 1310 nm
L_c = Cavity Length (air) ~ 30mm => 0.1ns cavity trip time
Resonant Cavity Modes are c/L_c = 10 GHz
Let f_Δ = 10 GHz
Frequency Steps/Sweep = $c/(L_c\ f_s)$ ~ 2,000
Total Frequency Sweep = $f_D = f_\Delta\ c/(L_c\ f_s)$ ~ 2.e13 Hz
Total Wavelength Sweep = $\lambda_S \sim \lambda_o^2\ f_\Delta/(L_c\ f_s)$ ~ 114 nm
f_s= Axial Sweep Frequency ~ 5 MHz

FIGURE 14

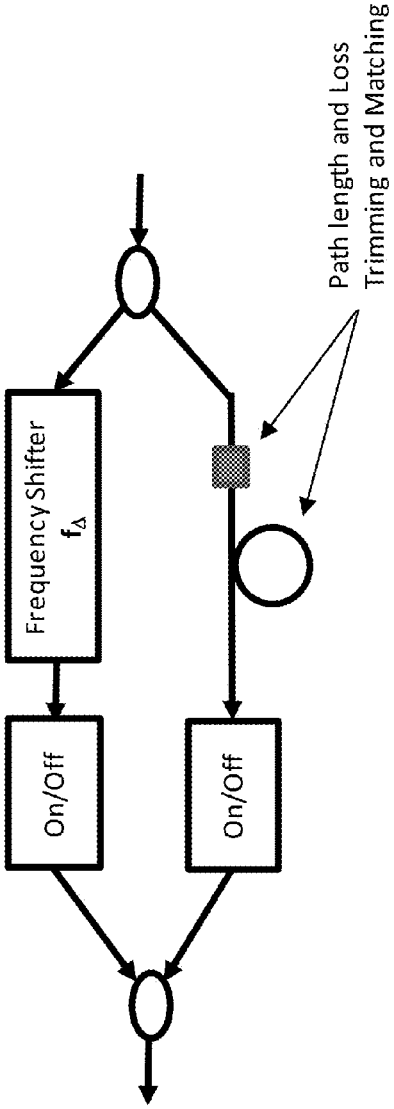
Path length and Loss
Trimming and Matching
Frequency Shifter
f_Δ
On/Off
On/Off
a)

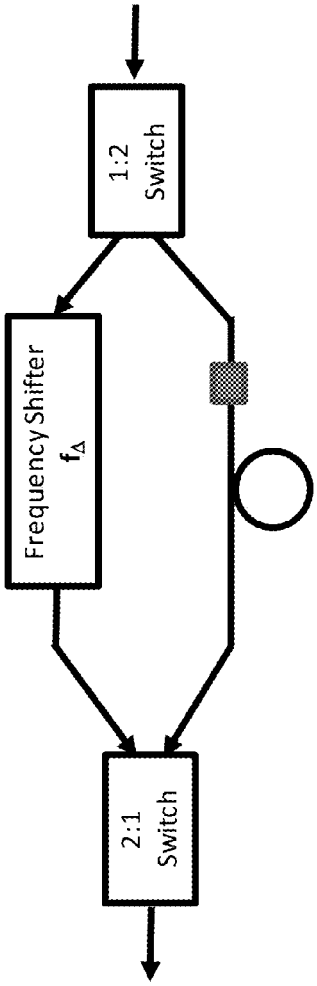
1:2
Switch
Frequency Shifter
f_Δ
2:1
Switch
b)

FIGURE 15

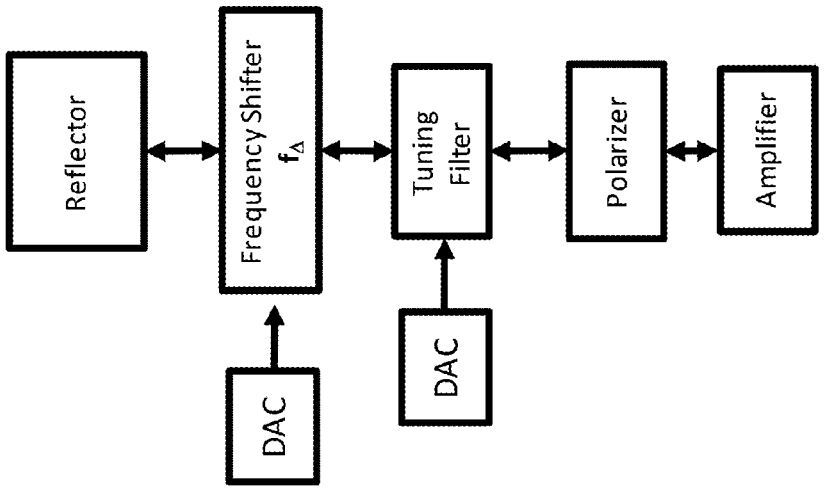
Reflector
Frequency Shifter
f_Δ
Tuning Filter
Polarizer
Amplifier
DAC
DAC

FIGURE 16

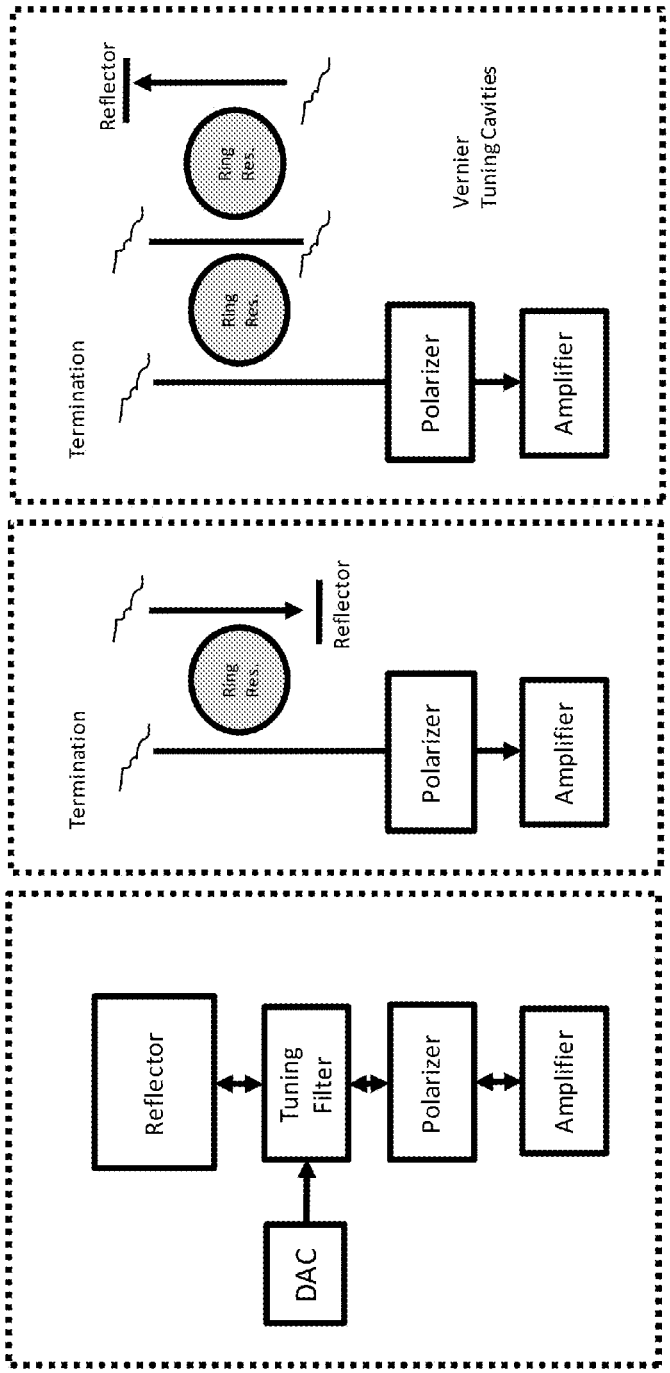
a)
Reflector
Tuning Filter
Polarizer
Amplifier
DAC
b)
Termination
Ring Res.
Reflector
Polarizer
Amplifier
c)
Termination
Ring Res.
Ring Res.
Reflector
Vernier Tuning Cavities
Polarizer
Amplifier

FIGURE 17

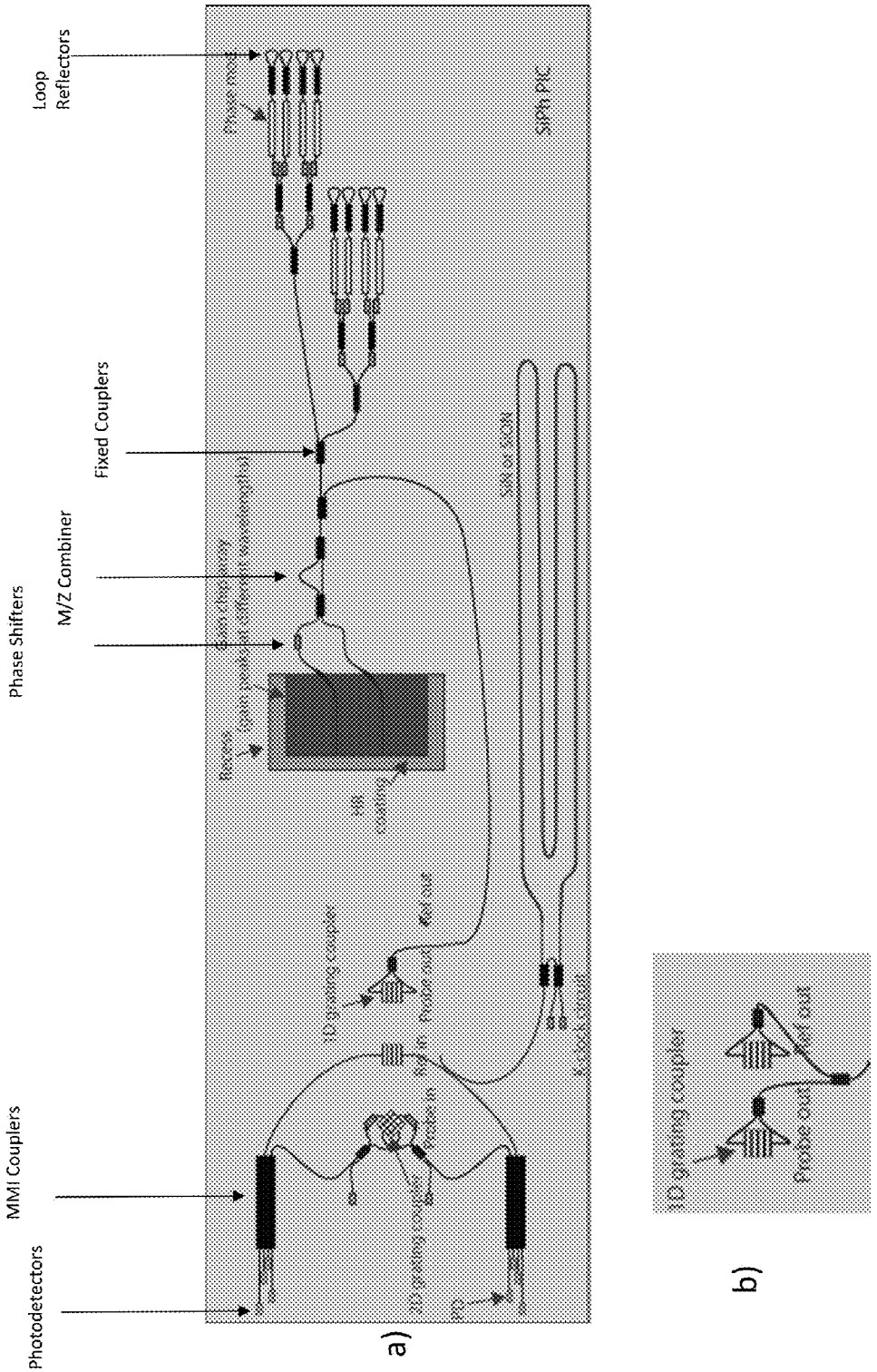
Loop Reflectors
Fixed Couplers
M/Z Combiner
Phase Shifters
MMI Couplers
Photodetectors
SiPh PIC
a)
b)

Figure 18

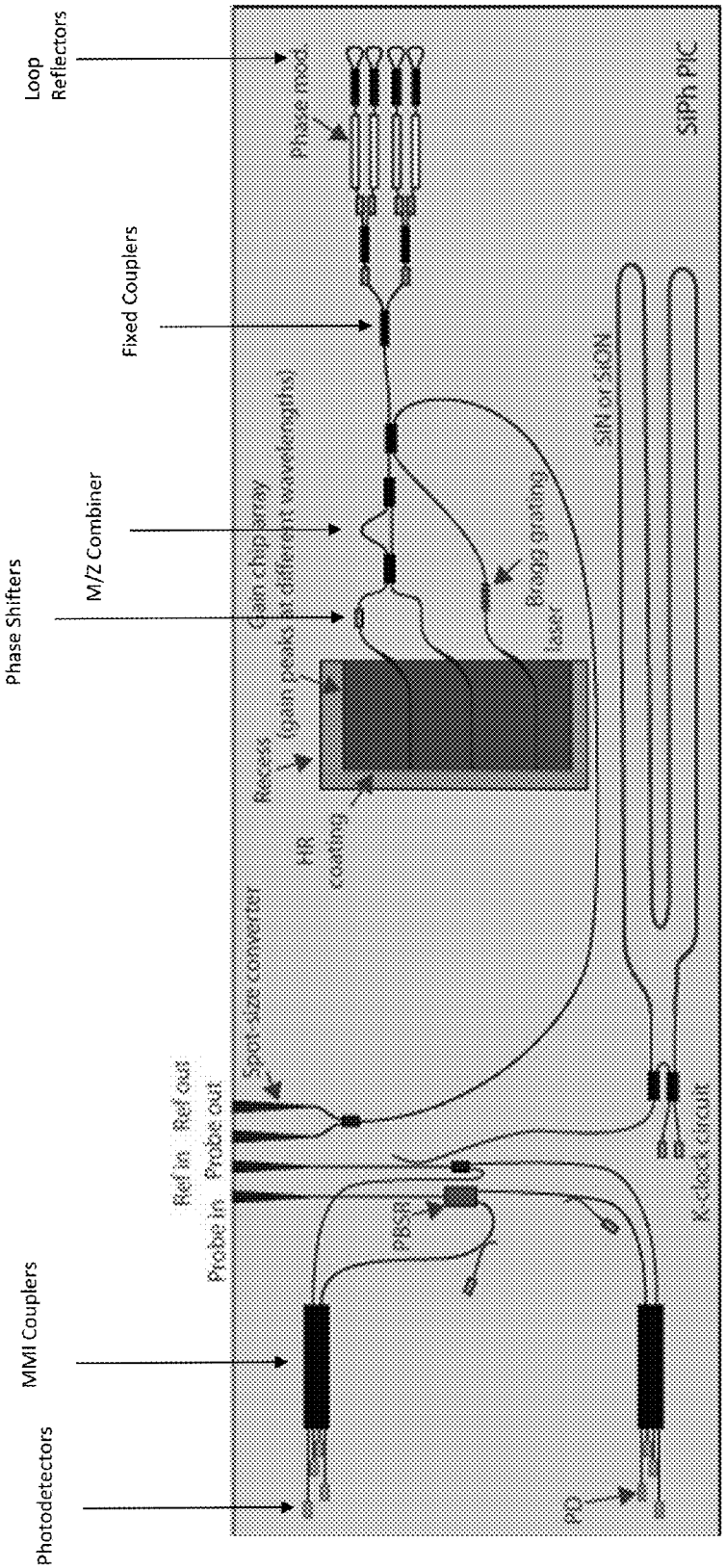
Loop Reflectors
Fixed Couplers
M/Z Combiner
Phase Shifters
MMI Couplers
Photodetectors
SiPh PIC
Phase mod
Ref in
Ref out
Probe in
Probe out
PBSR
PD

Figure 19

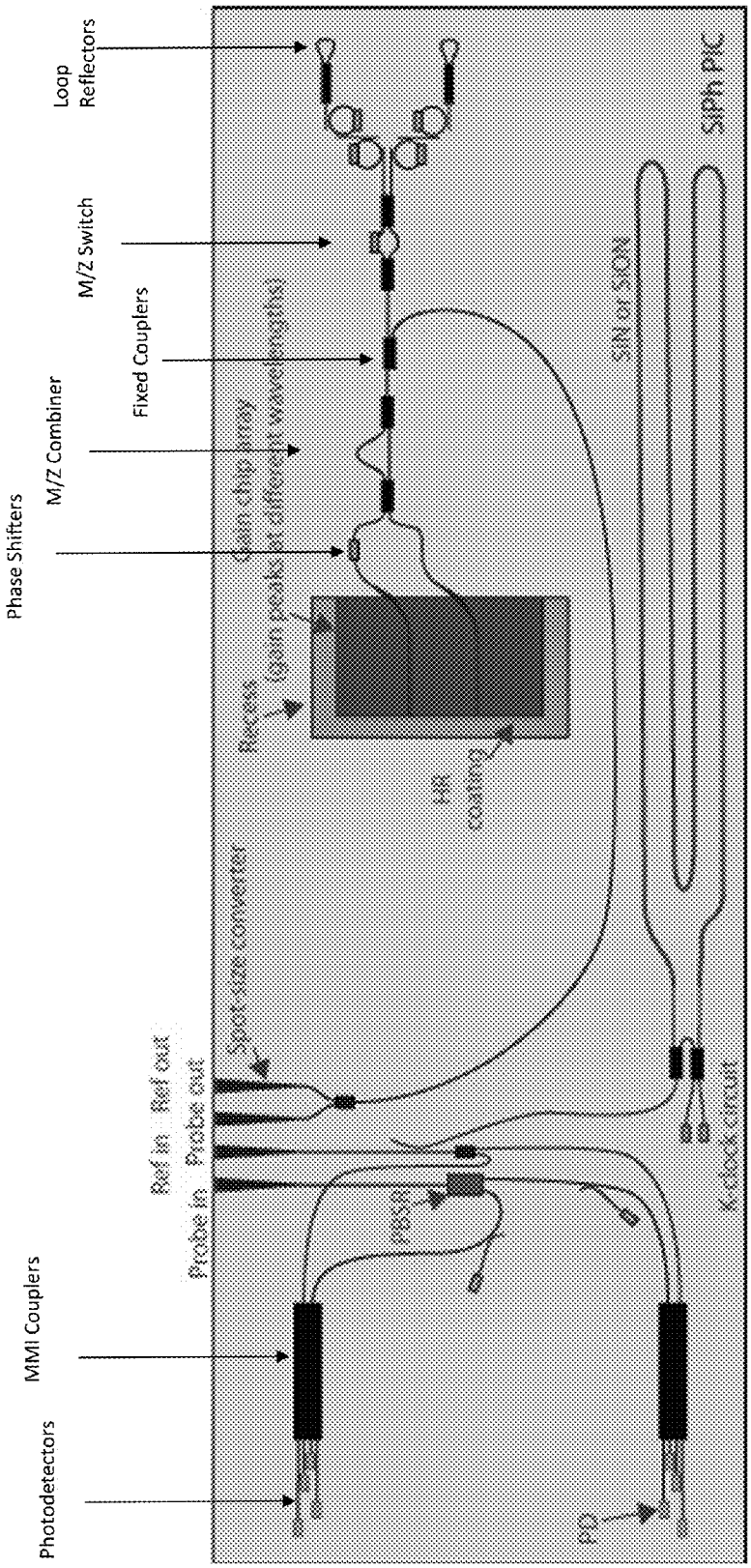
Loop Reflectors
M/Z Switch
Fixed Couplers
M/Z Combiner
Phase Shifters
MMI Couplers
Photodetectors
SiN or SiON
SiPh PIC
Ref in
Ref out
Probe in
Probe out
Spot-size converter
Resistor
PD
K-clock circuit

Figure 20

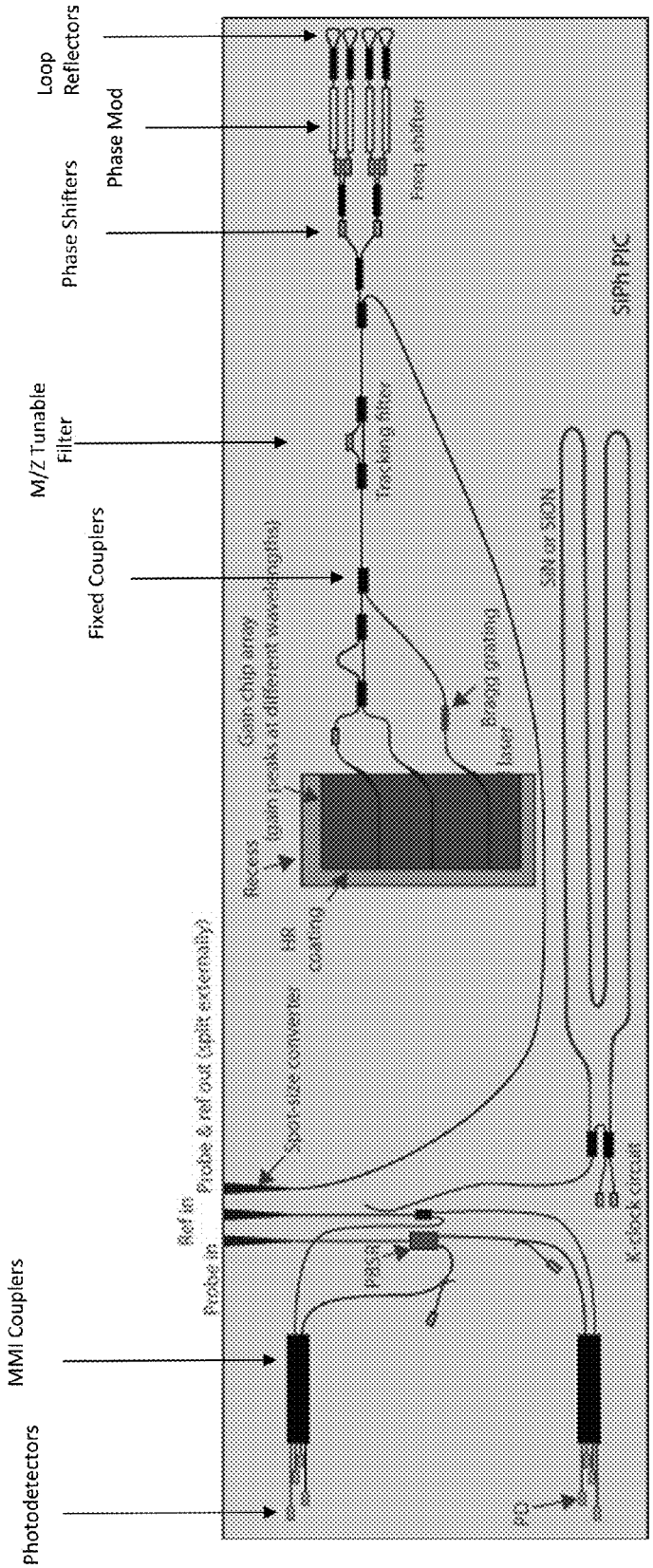
Loop Reflectors
Phase Mod
Phase Shifters
M/Z Tunable Filter
Fixed Couplers
MMI Couplers
Photodetectors
SiPh PIC

Figure 21

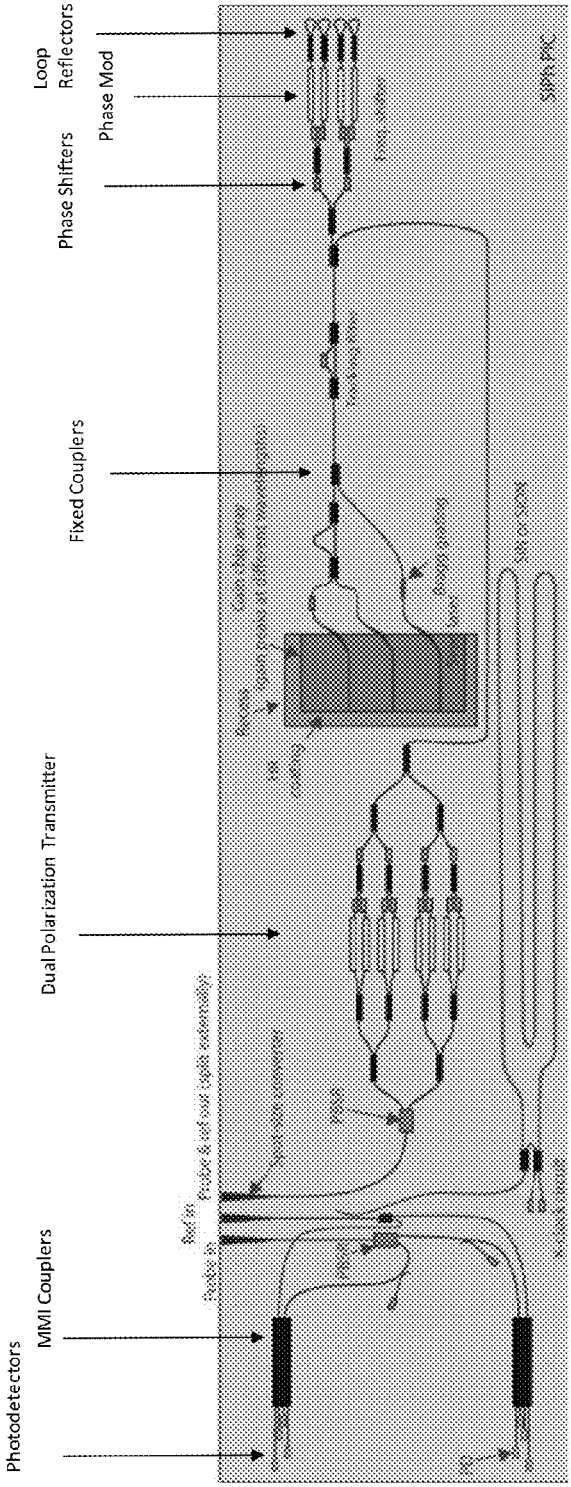
Loop Reflectors
Phase Mod
Phase Shifters
Fixed Couplers
Dual Polarization Transmitter
MMI Couplers
Photodetectors

FIGURE 22

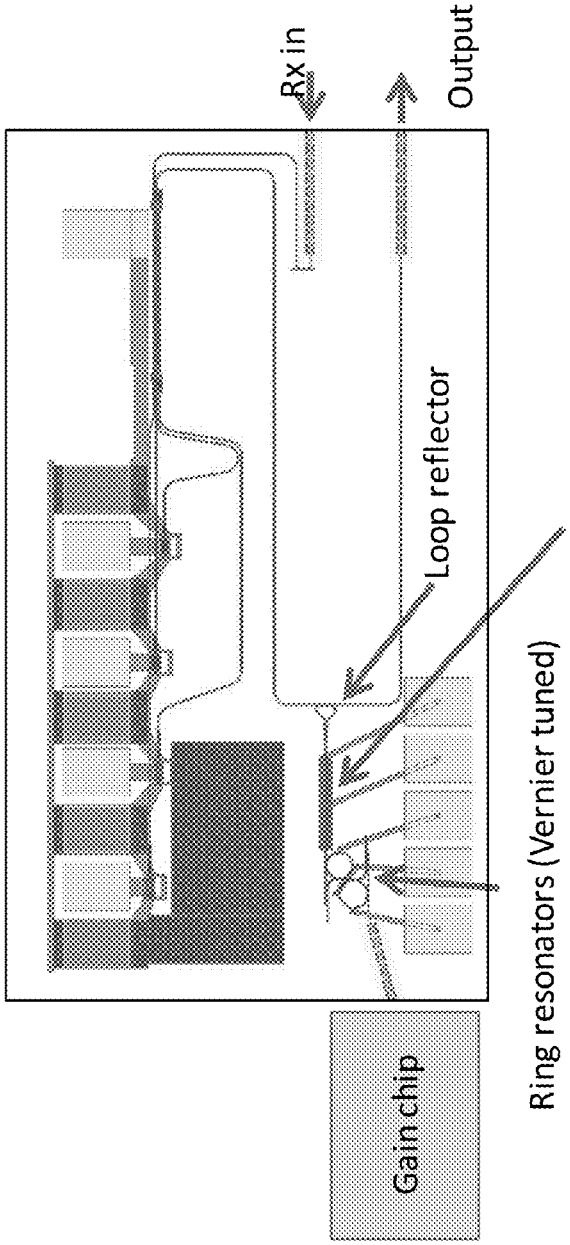
Rx in
Output
Loop reflector
Ring resonators (Vernier tuned)
Gain chip

FIGURE 23(a)

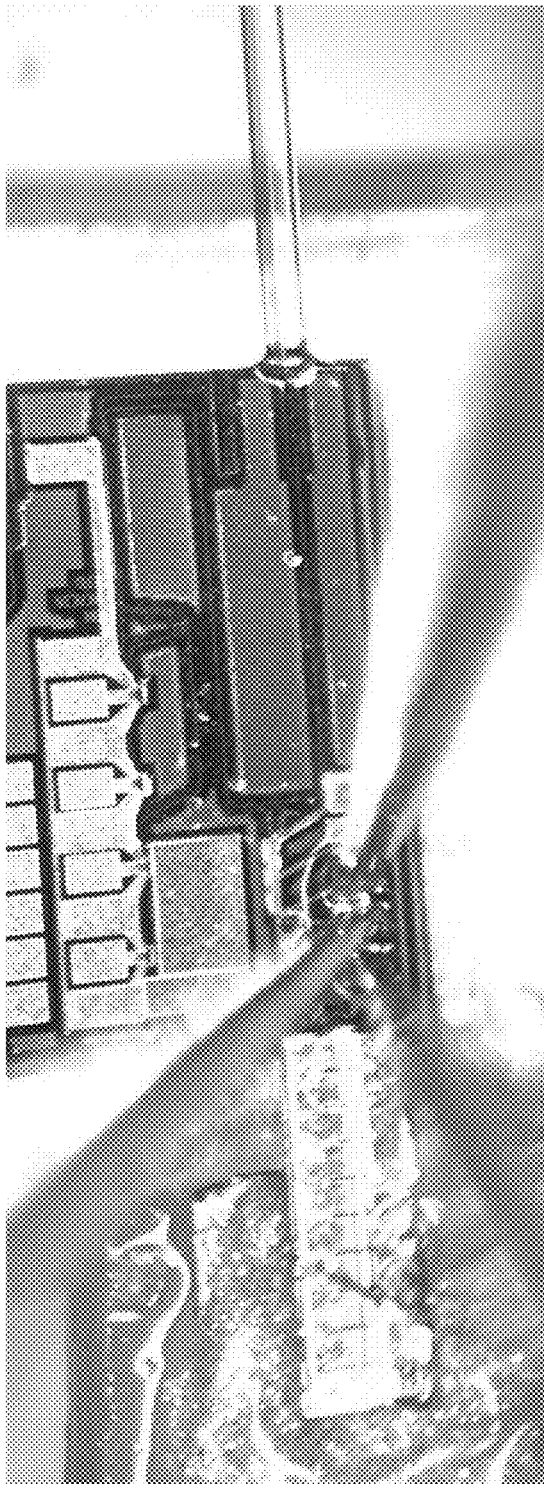

FIGURE 23(b)

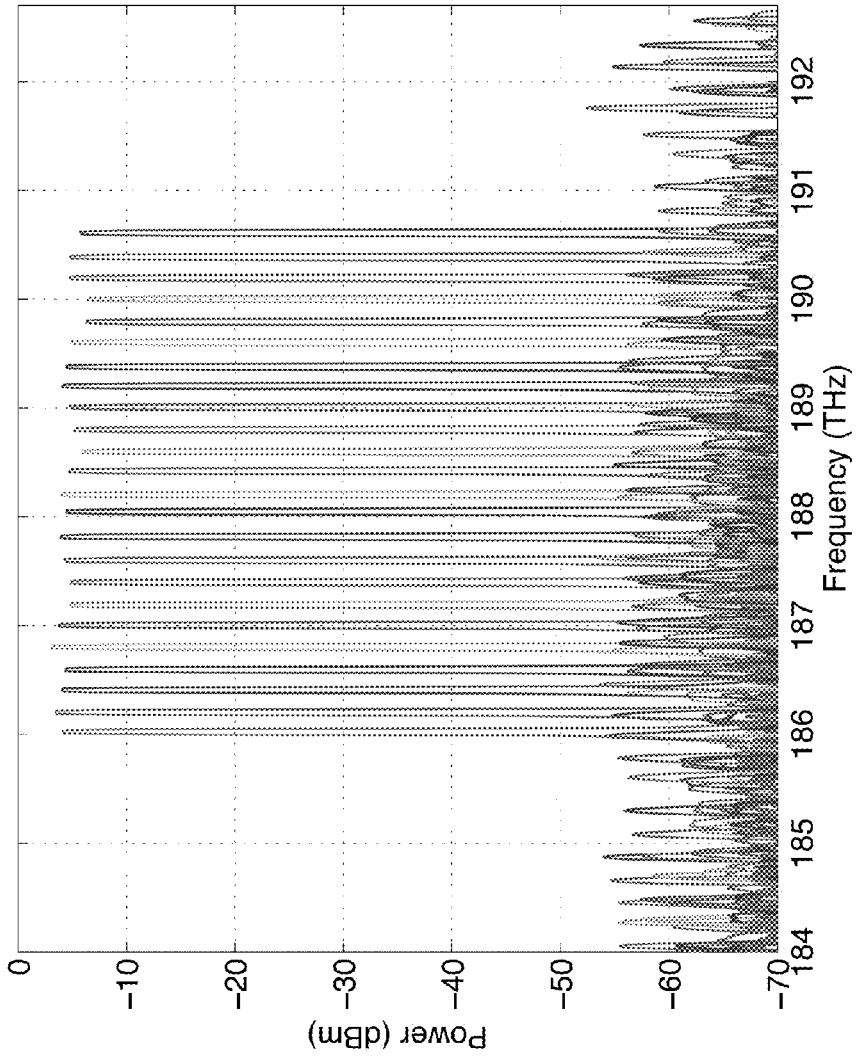
Power (dBm)
0
−10
−20
−30
−40
−50
−60
−70
184
185
186
187
188
189
190
191
192
Frequency (THz)

FIGURE 23(c)

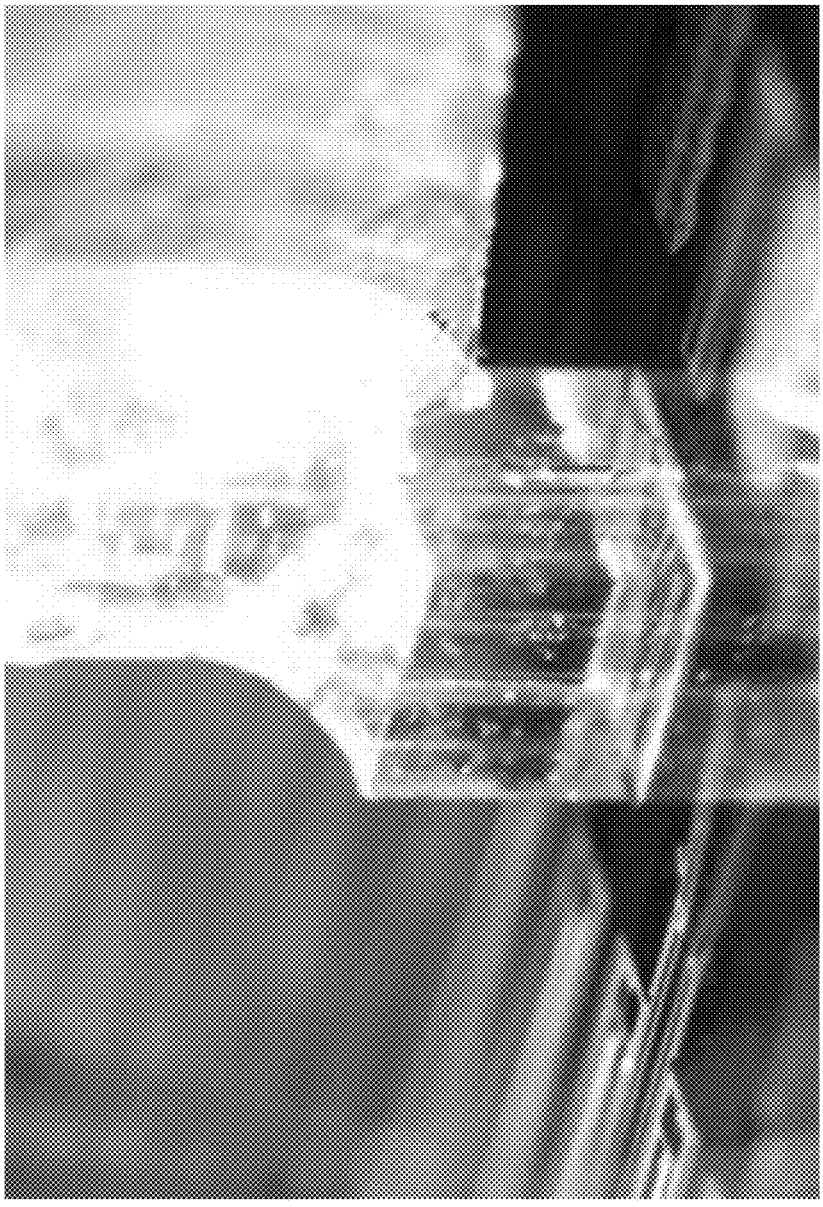

FIGURE 24

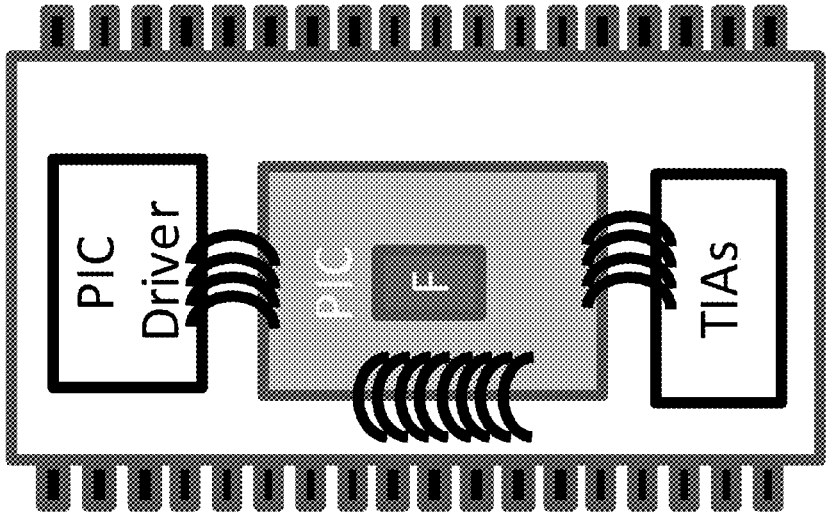

FIGURE 25(a)

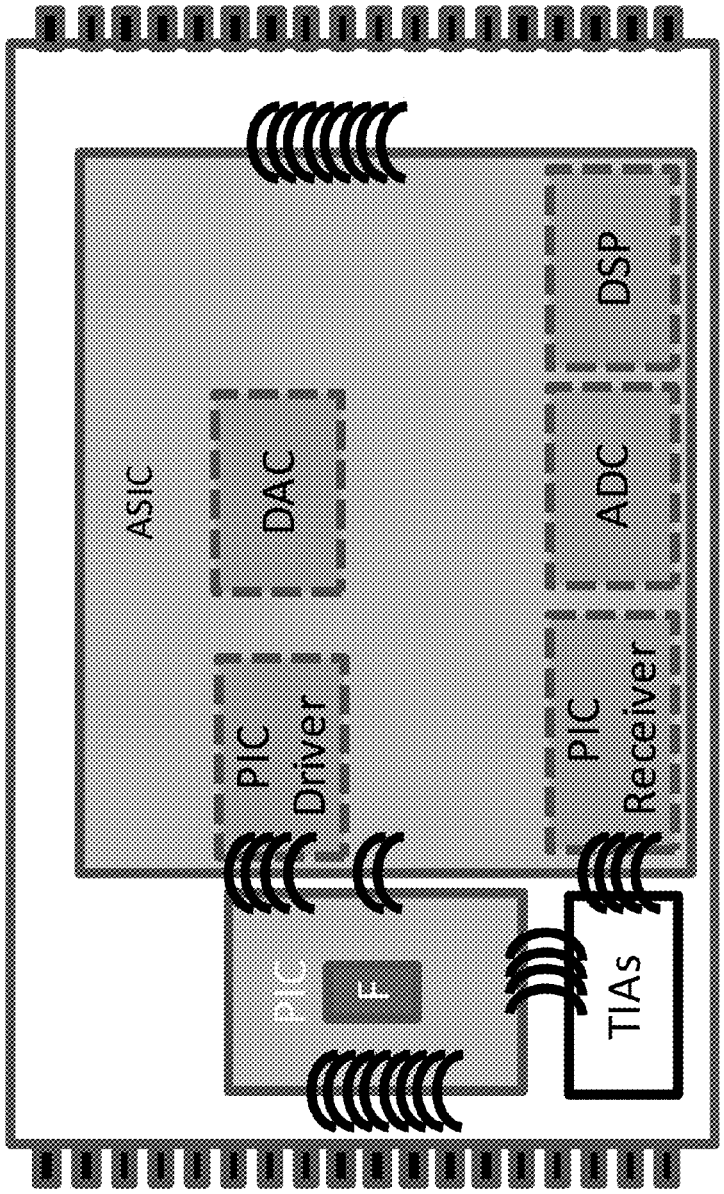

FIGURE 25(b)

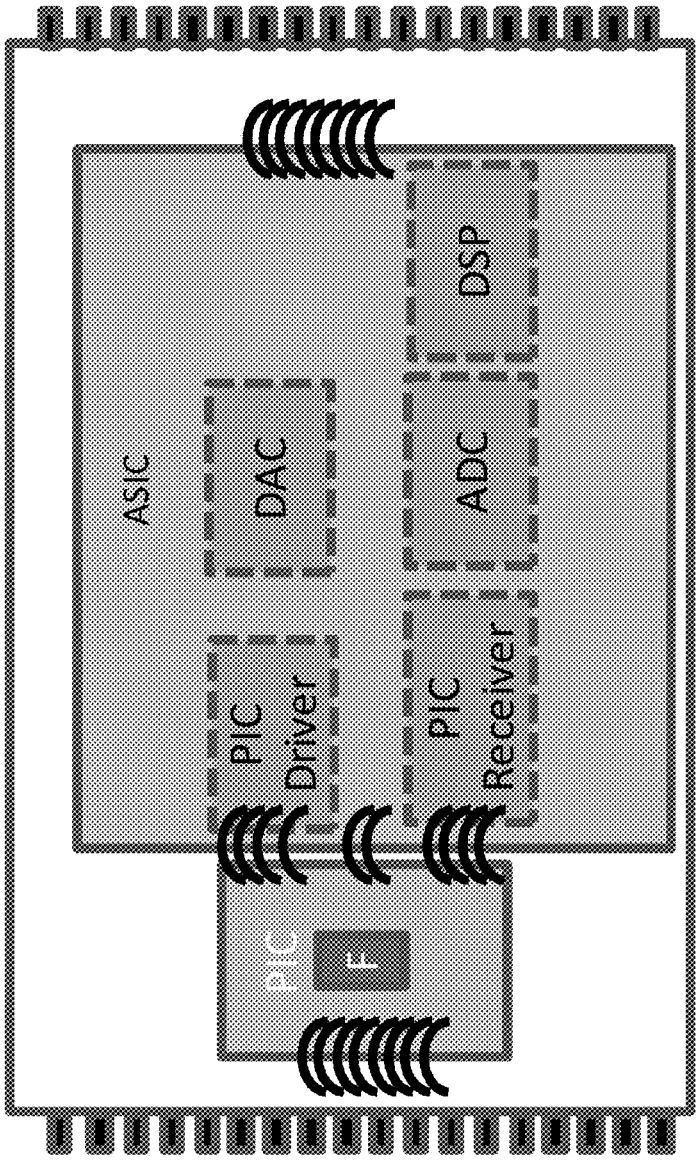

FIGURE 25(c)

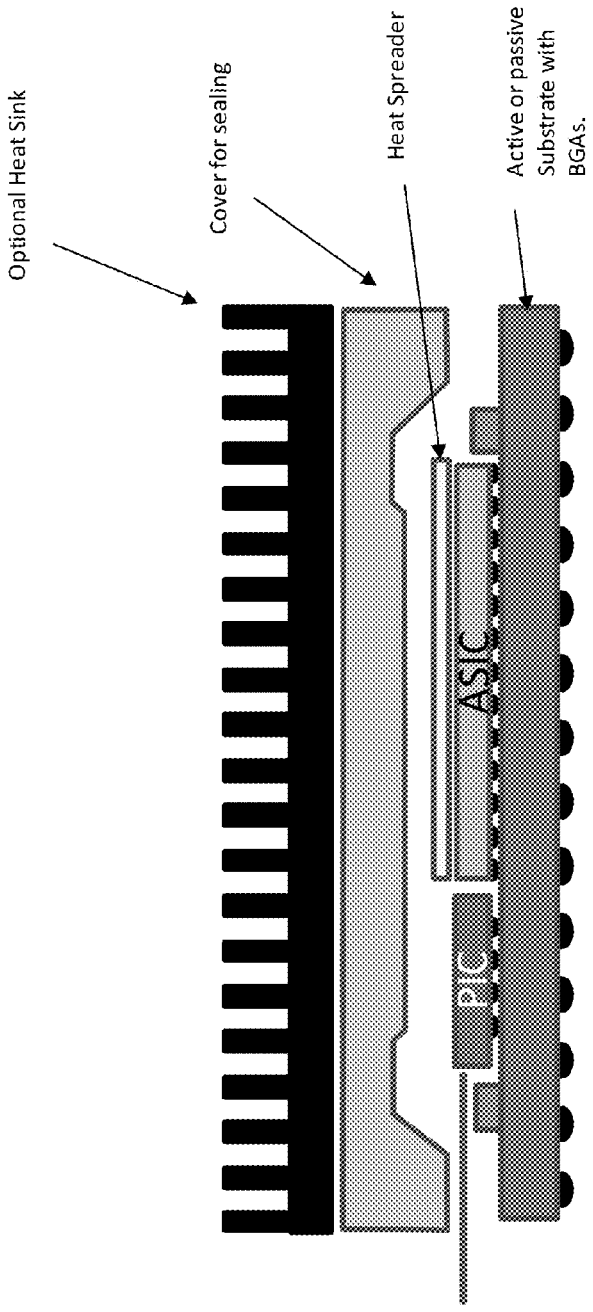
Optional Heat Sink
Cover for sealing
Heat Spreader
Active or passive Substrate with BGAs.
ASIC
PIC

FIGURE 26

INTEGRATED OPTICAL COHERENCE TOMOGRAPHY SYSTEMS AND METHODS

CROSS REFERENCE TO RELATED APPLICATION

This application claims the benefit of U.S. Provisional Patent Application Ser. No. 61/838,313 filed 23 Jun. 2013 which is incorporated by reference in its entirety as if set forth at length herein.

TECHNICAL FIELD

This disclosure relates generally to the field of optical signal acquisition, processing, and imaging. More particularly, this disclosure pertains to integrated optical coherence tomography systems, structures, and methods and related optical sensing, imaging, and ranging methods, systems and structures employing tunable optical sources and coherent detection.

BACKGROUND

Optical coherence tomography (OCT) is now known to be a minimally invasive optical imaging technique that provides high-resolution, cross-sectional images of tissues and turbid media and which can seamlessly integrates into other diagnostic procedures. OCT can provide real-time images of tissues in situ and can advantageously be used where conventional excisional biopsy is hazardous or impossible, to reduce sampling errors associated with conventional excisional biopsy, or to guide further interventional procedures. Given its exceptional promise, systems and methods for improved OCT, as well as ranging and imaging would represent a welcome addition to the art.

SUMMARY

An advance in the art is made according to an aspect of the present disclosure directed to integrated optical systems, methods and related structures employing tunable optical sources and coherent detection useful—for example—in OCT, ranging and imaging systems.

In contrast to contemporary, prior-art OCT systems and structures that employ simple, fiber optic or miniature optical bench technology using small optical components positioned on a substrate, systems and methods according to the present disclosure employ one or more photonic integrated circuits (PICs), use swept-source techniques, and employ a widely tunable optical source(s) and include multiple functions and in some embodiments all the critical complex optical functions are contained on one photonic integrated circuit.

An illustrative structure according to the present disclosure includes an interferometer that divides a tunable optical signal between a reference path and a sample path and combines optical signals returning from the reference path and the sample path to generate an interference signal, said interferometer including a dual polarization, dual-balanced, in-phase and quadrature (I/Q) detection outputs and integrated photodetectors and a detection system that detects the interference signal from which information about a longitudinal reflectivity profile of optical properties of a sample positioned in the sample path may be generated wherein the interferometer and the detection system are all integrated onto a single photonic integrated circuit (PIC). The optical information can eventually be represented in the form of a 1D, 2D, or 3D image. The detection system can be simple (e.g. a transimpedance amplifier (TIA)) or can include more complex electrical signal processing. The information

Further aspects of this illustrative structure according to an aspect of the present disclosure further includes a tunable optical source system that generates the tunable optical signal and/or a k-clock module for generating a k-clock signal for triggering the detector system wherein the k-clock, the interferometer, the tunable optical source system and the detection system are all integrated onto the PIC.

BRIEF DESCRIPTION OF THE DRAWING

A more complete understanding of the present disclosure may be realized by reference to the accompanying drawings in which:

FIGS. **1**(*a*)-**1**(*d*) show schematic diagrams illustrating (*a*) swept-source OCT concept, (*b*) example system specifications, (*c*) axial and lateral resolution, and (*d*) illustration of 1D, 2D, and 3D imaging from a series of axial scans according to an aspect of the present disclosure;

FIG. **2** shows a schematic block diagram of a system having a single dual-balanced receiver according to an aspect of the present disclosure;

FIG. **3** shows a schematic block diagram of a system having circulators and a 90 degree hybrid exhibiting dual-balanced I and Q channels according to an aspect of the present disclosure;

FIG. **4** shows a schematic block diagram of a system having circulators and dual polarization receiver with a polarization splitter and 90 degree hybrids exhibiting I and Q channels in two polarizations according to an aspect of the present disclosure;

FIG. **5** shows a schematic block diagram of a system having circulators and dual polarization receiver with a polarization splitter and 90 degree hybrids exhibiting I and Q channels in two polarizations and surface grating couplers used to couple light on and off a photonic integrated circuit (PIC) according to an aspect of the present disclosure;

FIG. **6** shows a schematic block diagram of a system having a single PIC input/output port and a dual polarization receiver with a polarization splitter and 90 degree hybrids exhibiting I and Q channels in two polarizations where the system has a laser with long coherence length and a delay for the reference arm contained within the single PIC according to an aspect of the present disclosure;

FIG. **7** shows a schematic block diagram of a system having couplers and dual polarization receiver including a polarization splitter and 90 degree hybrids exhibiting I and Q channels in two polarizations and a dual polarization modulator according to an aspect of the present disclosure;

FIG. **8** shows schematic block diagrams of three k-clock systems according to an aspect of the present disclosure;

FIGS. **9**(*a*)-**9**(*c*) show a schematic block diagrams illustrating *a*) a frequency tunable optical source including a ring configuration and optical frequency shifter; *b*) a frequency shift including a phase modulator and serrodyne modulation; *c*) a frequency shifter having two Mach Zehnder modulators according to an aspect of the present disclosure;

FIG. **10** shows an exemplary output of the frequency shifter of FIG. **9**(*c*) constructed in a PIC according to an aspect of the present disclosure;

FIGS. **11**(*a*)-**11**(*b*) show a schematic block diagrams illustrating two different methods for achieving a frequency shift as compared with that shown in FIG. **9**(*c*) and according to an aspect of the present disclosure;

FIG. **12** shows a schematic block diagram illustrating an exemplary Mach-Zehnder modulator employed as a filter in a tunable laser according to an aspect of the present disclosure;

FIG. **13** shows a schematic block diagram illustrating a ring laser configuration employing two frequency shifters according to an aspect of the present disclosure;

FIG. **14** shows a schematic block diagrams illustrating a ring laser configuration having a frequency shifter and an optional tracking filter wherein the frequency shifter is configured to shift light entering into it to a new frequency that is closely aligned with a ring cavity mode according to an aspect of the present disclosure;

FIGS. **15**(*a*)-**15**(*b*) show a schematic block diagrams illustrating two different embodiments of a frequency shifter wherein a reconfigurable light modulator is employed and another exhibiting either frequency shift or pass-through according to an aspect of the present disclosure;

FIG. **16** shows a schematic block diagram illustrating alternate laser embodiments that employ a linear cavity configuration in close electrical communication with one or more DACs to achieve high speed according to an aspect of the present disclosure;

FIGS. **17**(*a*)-**17**(*c*) show a schematic block diagrams illustrating alternate laser embodiments that do not include a frequency shifter in a cavity including one ring resonator configuration and a two ring resonator configuration according to an aspect of the present disclosure;

FIGS. **18**(*a*)-**18**(*b*) show schematic block diagrams illustrating a silicon PIC having an embedded gain chip and surface grating couplers and multiple phase modulators that can act as separate frequency shifters or impart other optical modulation within the laser cavity; **18**(*a*) illustrates an example including one output surface grating coupler while **18**(*b*) illustrates an example including two output surface grating couplers according to an aspect of the present disclosure.

FIG. **19** shows a schematic block diagram illustrating a silicon PIC with an embedded gain chip and end face coupling and a frequency shifter according to an aspect of the present disclosure;

FIG. **20** shows a schematic block diagram illustrating a silicon PIC with an embedded gain chip employing end-face coupling and two sets of ring laser resonators according to an aspect of the present disclosure;

FIG. **21** shows a schematic block diagram illustrating a silicon PIC with an embedded gain chip employing end-face coupling and wherein the laser has a tunable tracking filter and a an arbitrary modulator that can impart phase, frequency, or amplitude modulation on light within the laser cavity according to an aspect of the present disclosure;

FIG. **22** shows a schematic block diagram illustrating a silicon PIC similar to that shown in FIG. **21** wherein the PIC includes a dual polarization I/Q modulator such as that shown in FIG. **7** according to an aspect of the present disclosure;

FIGS. **23**(*a*)-**23**(*c*) show a schematic block diagrams illustrating a tunable laser transmitter and single polarization I/Q coherent receiver constructed on a single PIC including schematic, **23**(*a*); photograph, **23**(*b*); and sample output of tunable laser spectrum, **23**(*c*); according to an aspect of the present disclosure;

FIG. **24** shows a schematic block diagram illustrating a fiber assembly including three single mode optical fibers coupled to three surface grating couplers on a silicon PIC according to an aspect of the present disclosure;

FIGS. **25**(*a*)-**25**(*c*) show schematic block diagrams illustrating a PIC packaged with various electronic components according to an aspect of the present disclosure; and

FIG. **26** shows a schematic block diagram illustrating an exemplary PIC and electronic circuit on a carrier substrate according to an aspect of the present disclosure;

DETAILED DESCRIPTION

The following merely illustrates the principles of the disclosure. It will thus be appreciated that those skilled in the art will be able to devise various arrangements which, although not explicitly described or shown herein, embody the principles of the disclosure and are included within its spirit and scope. More particularly, while numerous specific details are set forth, it is understood that embodiments of the disclosure may be practiced without these specific details and in other instances, well-known circuits, structures and techniques have not be shown in order not to obscure the understanding of this disclosure.

Furthermore, all examples and conditional language recited herein are principally intended expressly to be only for pedagogical purposes to aid the reader in understanding the principles of the disclosure and the concepts contributed by the inventor(s) to furthering the art, and are to be construed as being without limitation to such specifically recited examples and conditions.

Moreover, all statements herein reciting principles, aspects, and embodiments of the disclosure, as well as specific examples thereof, are intended to encompass both structural and functional equivalents thereof. Additionally, it is intended that such equivalents include both currently-known equivalents as well as equivalents developed in the future, i.e., any elements developed that perform the same function, regardless of structure.

Thus, for example, it will be appreciated by those skilled in the art that the diagrams herein represent conceptual views of illustrative structures embodying the principles of the invention.

In addition, it will be appreciated by those skilled in art that any flow charts, flow diagrams, state transition diagrams, pseudocode, and the like represent various processes which may be substantially represented in computer readable medium and so executed by a computer or processor, whether or not such computer or processor is explicitly shown.

In the claims hereof any element expressed as a means for performing a specified function is intended to encompass any way of performing that function including, for example, a) a combination of circuit elements which performs that function or b) software in any form, including, therefore, firmware, microcode or the like, combined with appropriate circuitry for executing that software to perform the function. The invention as defined by such claims resides in the fact that the functionalities provided by the various recited means are combined and brought together in the manner which the claims call for. Applicant thus regards any means which can provide those functionalities as equivalent as those shown herein. Finally, and unless otherwise explicitly specified herein, the drawings are not drawn to scale.

Thus, for example, it will be appreciated by those skilled in the art that the diagrams herein represent conceptual views of illustrative structures embodying the principles of the disclosure.

More specifically, much of the discussion that follows is presented with respect to a swept-source optical coherence tomography system. However, those skilled in the art will

readily appreciate that this discussion is broadly applicable to a wide range of applications that employ on a swept laser (or other optical sources that may be rapidly swept over a wide frequency range) and interferometric electro-optical detection, for example, ranging, medical imaging, non-destructive evaluation and testing, laser radar, spectroscopy, and communications—among others.

Turning now to FIGS. **1**(*a*)-**1**(*d*), and in particular FIG. **1**(*a*), there is shown a schematic of the axial imaging component of an optical coherence tomography arrangement including a swept-source according to an aspect of the present disclosure. More particularly in that FIG. **1**(*a*), a frequency swept light source is coupled to a Michelson interferometer which comprises two optical paths or "arms". Those skilled in the art will appreciate that while a Michelson interferometer is shown in the illustrative examples described herein other types of interferometers are also possible and are contemplated by this disclosure.

One arm of the Michelson interferometer comprises a reference optical path having a mirror which reflects light and the other arm comprises a sample optical path into which is positioned a sample whose axial/longitudinal reflectivity profile is to be measured. Operationally, light collected from both the reference and sample paths are interferometrically combined and directed to a photodetector (including subsequent signal processing not specifically shown). Due to a delay between reference and sample reflections, interferometric detection and frequency sweep of a laser light source, the photodetector output includes information about the axial/longitudinal reflectivity profile of the sample that may be advantageously extracted by Fourier Transform (FT) techniques or other techniques as known in the art. As may be readily appreciated, a number of architectures and arrangements applying these broad techniques are possible. Exemplary and/or illustrative architectures and arrangements are contemplated and presented by this disclosure.

More particularly, other types of swept-source, optical coherence tomography (SS-OCT) system topologies that are known in the art are contemplated by this disclosure. With reference to FIG. **1**(*b*), there are shown exemplary, illustrative specifications for systems constructed according to aspects of the present disclosure. In particular, center wavelength(s) ~1310 nm; Scan Range(s) >100 nm; Coherence Length(s) >20 mm; Sweep Speed(s) >100 kHz; Laser Output Power(s) >25 mW; and Ideal Sweep(s) exhibiting 100% duty cycle sawtooth—are all (as well as others) are contemplated by this disclosure. Note that these exemplary, illustrative specifications are in no way limiting. It is understood and those skilled in the art will readily appreciate that there are a wide variety of other specifications contemplated such as different center wavelength(s), sweep speed(s), etc., contemplated by this disclosure as well.

With reference to FIG. **1**(*c*), there it depicts in schematic form an aspect of contemporary SS-OCT systems namely, that the longitudinal resolution of such systems is substantially dictated by properties of the optical source (i.e., its spectral bandwidth) and the focusing properties of light onto/into the sample. More particularly, the schematic diagram of FIG. **1**(*c*) shows interrelationships between axial resolution, transverse resolution, depth of field as they relate to systems exhibiting low numerical aperture focus (NA) and high NA focus. As may be appreciated, for many contemporary OCT systems, it is the optical spectral bandwidth of the source that is the limiting factor of its longitudinal resolution.

FIG. **1**(*d*) shows one example in schematic form of how 1D, 2D, 3D images may be constructed by combining axial/longitudinal scanning from a laser source frequency sweep and Fourier transform processing along with lateral or rotational scanning of light onto a sample via a probe module (not specifically shown) as performed by contemporary systems. One can then implement lateral, rotational, or transverse scanning to product 2D and 3D images. Other configurations of SS-OCT systems employing parallel acquisition systems are variations to these contemporary systems.

As previously noted—and in sharp contrast to contemporary, prior-art SS-OCT systems and structures—systems and structures according to the present disclosure employ one or more photonic integrated circuits (PICs) that are advantageously constructed using combinations of optically compatible material such as Silicon (Si), Indium Phosphide (InP), Gallium Arsenide (GaAs), Indium arsenide (InAs) quantum dots, Germanium (Ge), or other suitable, optically compatible material. Of further contrast, prior art OCT systems, such as those that do describe photonic integrated circuits, often times do not utilize swept-source techniques, but instead use a very different OCT technology namely, spectral domain optical coherence tomography. And for those prior art systems that do describe the use of PICs for SS-OCT they do not address the integration of many optical functions such as interferometers, dual polarization, dual balanced, I/Q receivers with integrated photo-detectors and electro-optical integration which is key to making this systems robust, manufacturable, small, and low-cost. Finally, prior art OCT systems generally employ simple, miniature optical bench technology using small optical components placed on a substrate, and do not include a widely tunable optical source or integrated k-clocks and detectors.

With these principles in place, we may now examine more particular exemplary configurations and systems according to aspects of the present disclosure. Turning now to FIG. **2**, there it shows a schematic block diagram of an illustrative system having a single, dual-balanced receiver according to an aspect of the present disclosure. As depicted therein, a dotted line outlines those components that may be advantageously incorporated (integrated) into/onto a single PIC as one exemplary configuration according to the present disclosure. Importantly, and as may be readily appreciated by those skilled in the art, a greater or lesser number of the components shown may be integrated into the PIC as system design dictates or further benefit(s) arise from such integration. For example in some illustrative embodiments the transmit laser can be located outside the PIC.

As shown in that FIG. **2**, a tunable (transmit) laser is optically coupled to a 90/10 coupler. The 90% output of that coupler is directed to a 50/50 coupler, the output of which is directed to a probe module that couples light to/from a sample while—in a preferred embodiment—performing a lateral or a rotational scanning of light across the sample. Note that in this schematic FIG. **2**, the lateral scanning is not specifically shown.

Returning to FIG. **2**, the 10% output of the 90/10 coupler is directed to an 80/20 coupler that further couples light to and from a reference module. As may be readily appreciated, such a reference module may include an fixed or adjustable path length device that sets measurement range of interest and include other devices (e.g., polarization rotators, attenuators, lenses, mirrors, etc.) and perform other functions as well. Unused ports of the 50/50 sample path and the 80/20

reference path may be terminated or may alternatively be used to supply light to a k-clock input port.

As shown further in FIG. **2**, light reflected back from the 80/20 coupler is shown coupled to a second 90/10 coupler. The 10% output of that second 90/10 coupler is shown coupled to an optional k-clock and detector—which will be discussed later—and the 90% output of that second 90/10 coupler is shown coupled to an optional polarization controller that may be automatically or manually adjusted. Notably, it may be advantageous to include another polarization controller and 90/10 coupler in the sample path to balance dispersion and birefringence.

As may be appreciated, the polarization controller so used may be an active controller that is controlled by the electronics module (connections not specifically shown) or alternatively, be manually set. Reference and sample light are coupled to a 50/50 receiver coupler and directed to a balanced photo-detector configuration to enhance receiver sensitivity and minimize laser intensity noise as well as other noise sources.

Output from the photo-detector is directed into an electrical processing module that may advantageously include one or more transimpedance amplifiers (TIAs), Analog-to-Digital Converter, (ADCs), Digital to Analog Converter(s), DACs, and Digital Signal Processing (DSP) electronic modules. Advantageously, such electronic modules may be included in one or more integrated electronic chips including Application Specific Integrated Circuits (ASICs) and/or Field Programmable Gate Arrays (FGPAs) as well as other discrete or monolithic electronic devices. This electrical processing in some embodiments can be housed in the same electro-mechanical package (co-packaged) or can be located in a separate electromechanical package.

As shown, the electrical module depicted in FIG. **2** also receives the k-clock output and is further connected to the transmit laser such that it may control its operational characteristics. Some exemplary embodiments do not require the use of a k-clock but it is advantageous if the frequency sweep is not linear or highly repeatable as discussed later. As may be appreciated and understood, sections of the PIC shown in FIG. **2** and external to the dotted line may be optical fibers or free-space optical links or a combination thereof.

It is worth noting at this point in the discussion that a wide variety of other coupling ratios and configurations other than those shown are contemplated and consistent with this disclosure. For example, an alternative embodiment may replace the 50/50 and 80/20 output couplers (connecting the sample and references) with circulators such that an increase in useful signal power and an increase in the isolation of reflected light with respect to the laser cavity is achieved. In configurations where bulk circulators are used, four external connections to the PIC instead of the two shown in FIG. **2** are employed.

Turning now to FIG. **3**, there it shows a schematic block diagram of an illustrative system having circulators in place of the 50/50 and 80/20 splitters of FIG. **2**, and a 90 degree hybrid exhibiting dual-balanced I and Q channels according to an aspect of the present disclosure. More specifically, and as shown in FIG. **3**, received optical signals are routed to a 90 degree hybrid processor that includes four output signals that represent two dual-balanced in phase (I_x) and quadrature (Q_x) optical signals. The 90-degree hybrids may be—for example—multimode interference couplers, star couplers, or a network of 1×2 and 2×2 couplers.

The I (I_x) and Q (Q_x) signals depicted in FIG. **3** allow phase-sensitive detection of light from the sample and extraction of additional optical information on the sample and other signal processing improvements. Of further advantage, the photodetectors may be monolithically integrated into the PIC using a suitable optical detector material (e.g., Ge).

In one illustrative embodiment—and as may be readily appreciated by those skilled in the art—the photodetectors may be butt coupled or otherwise optically coupled to the PIC or located on a separate device. In the illustrative embodiment depicted in FIG. **3**, the entire region shown within dotted lines is advantageously included in/on one single PIC. In other contemplated embodiments according to the present disclosure, the tunable laser may be external to the PIC. Alternatively, only the receiver portion may be included within the PIC, or the circulators may be replaced with couplers and located within the PIC as well. As may be appreciated, a great number of configurations are contemplated by the present disclosure.

FIG. **4**, FIG. **5**, and FIG. **6** show further illustrative extensions to these configurations shown and described. More particularly, they depict illustrative configurations wherein a received optical signal is routed to a polarization diversity receiver that includes two 90-degree hybrid processors. Such embodiments advantageously exhibit improved capabilities with respect to polarization-diversity and polarization-sensitivity along with an improved ability to measure both the sample birefringence and other characteristics along with phase sensitive detection within each polarization. Such phase and polarization sensitive detection permits functional imaging via Doppler, increased sensitivity and improvements in signal processing and sample imaging information possibilities such as polarization independent imaging or polarization sensitive imaging.

FIG. **4** shows a schematic block diagram of an illustrative system including circulators and a dual polarization receiver including polarization splitters and 90 degree hybrids exhibiting I and Q channels in two polarizations according to an aspect of the present disclosure. As may be appreciated, such a system may be integrated onto a single PIC including source(s), k-clock, polarization controller, and dual polarization receiver.

FIG. **5** shows a schematic block diagram of an illustrative system having circulators and dual polarization receiver with a polarization splitter and 90 degree hybrids exhibiting I and Q channels in two polarizations and surface grating couplers used to couple light on and off a photonic integrated circuit (PIC) according to an aspect of the present disclosure. As depicted therein, the polarization controller is integrated, however this device is optional and may be included external to the PIC in the reference arm—or not at all. Alternatively—in those environments in which the bandwidth is very large—it may be beneficial to have a polarization controller positioned in both the sample and reference paths such as that shown thereby balancing particular optical properties such as birefringence, dispersion, and/or other optical characteristics.

With continued reference to FIG. **5**, it is noted that phase and polarization sensitive detection advantageously allows functional imaging via Doppler, increased sensitivity, and improvements in signal processing and sample imaging information capability such as polarization sensitive detection and imaging.

With continued reference to FIG. **5**, it is noted that the illustrative embodiment shown therein is compatible with surface grating couplers (SGC). As may be appreciated, one dimensional (1D) surface grating couplers may be used to direct (couple) light off of the PIC and into circulator(s)

while two dimensional (2D) surface grating couplers may be used to receive reflected light from the circulators and simultaneously split them into nearly orthogonal polarizations. As depicted in FIG. **5**, power monitors (PM) are used to monitor polarization alignment and other conditions of the reference path. Advantageously, wide-band grating couplers can be made by using a core material with a lower index than silicon, such as silicon nitride, and/or by using a smaller spot size on the grating, for example from a small core fiber. Of further advantage, different combinations of couplers or combinations of 1D and 2D couplers may be used simultaneously in alternative embodiments.

With reference now to FIG. **6**, there it shows an alternative embodiment according to an aspect of the present disclosure that particularly useful when used with a laser source having sufficiently long coherence length for the sample measurement distances. As depicted in FIG. **6**, the entire reference path length may be located on the PIC. Consequently, only one PIC external connection is employed—the one to the sample. With a configuration such as that depicted in FIG. **6**, an on-chip path delay unit constructed from a tightly wound spiral or other waveguide structure may be included. To impart low loss and low temperature dependence such a waveguide structure may be fabricated from Silicon Nitride (SiN) or Silicon Oxynitride (SiON) materials.

At this point we note that for improved axial/longitudinal resolution, it is important that each arm exhibit substantially matching total dispersion and birefringence characteristics. In certain configurations it is convenient to position/place similar devices in both arms so as to keep the optical characteristics balanced. For configurations in which such placement of similar structures is impossible or impractical, then one can—for example—introduce (additional) dispersion into the PIC structure by using—for example—ring resonators (as all-pass filters) coupled to waveguides. Advantageously as an alternative, if the path characteristics are not matched then it is also possible—if the coherence length of the laser is long and the optical properties are stable—to electronically post process this dispersion or birefringence imbalance out electronically in the DSP in cases where both I and Q phase sensitive detection is utilized.

Turning now to FIG. **7**, there it shows an alternative illustrative embodiment according to the present disclosure in which a transmitter path (the output laser light before the probe/sample) includes a dual polarization modulator and only one output light path from the PIC (the sample and probe module are split external to the PIC). As may be appreciated, the modulator in this embodiment may provide alternating on/off or other modulation (e.g. within an axial scan or sending alternate polarizations on adjacent axial scans) into the sample such that birefringence information along the axial profile of the sample is extracted. That is to say the modulation may be performed rapidly—relative to a laser frequency sweep time—or may be performed more slowly, alternatively on each laser sweep or other combinations.

In addition to the functionality described above, the modulator may also be used to set arbitrary intensity and phase information on each polarization such that the receiver module can perform processing on this modulation to extract additional features. For example a Hamming or other window can be applied to the laser output amplitude. As discussed earlier it is possible to locate the tunable optical transmit laser (or an equivalently functioning tunable optical source (e.g. and ASE source and a tunable filter)) external to the PIC. The polarization combiner after the two modulators may be either a 2D grating coupler or a polarization rotator and polarization beam combiner connected to a facet coupler.

At this point we note that polarization splitters, combiners, and rotators shown in the various figures are preferably fabricated onto the PIC and exhibit a broad bandwidth, low loss and high extinction characteristics. As those skilled in the art will readily appreciate, there are known a variety of ways to build such individual structures and devices.

With respect to surface grating couplers, there exist a variety of designs of surface grating couplers—including 1D and 2D grating couplers as well as designs exhibiting various fiber incidence (i.e., normal, slight, extreme)—such that output light is primarily coupled into two output waveguides instead of four, for example. As may be appreciated, one advantage of surface grating couplers is they are easy to fabricate and easy to couple light into/out of them. Also surface grating couplers eliminate the need to rotate polarization on the PIC, because both polarization (states) signals in the fiber maintain the same polarization in the PIC. Conversely, one disadvantage of using surface grating couplers is that it is difficult to make them such that they exhibit both a very broad bandwidth a very low loss.

With respect to polarization controller(s) shown in various figures, they too can be implemented in a variety of ways and exhibit a number of particular characteristics. By way of non-limiting example(s), it is noted that a polarization controller needs to exhibit a broad bandwidth and low loss. Also, the polarization controller should not introduce significant dispersion or birefringence over the laser tuning band. If such dispersion or birefringence exists then a second matching polarizer can be added—for example—to the sample arm of the system.

Advantageously, "endless" polarization controllers or resettable polarization controllers may be fabricated within the PIC, using, for example, a cascade of Mach-Zehnder interferometers. Alternatively, such polarization controllers may be located outside or off of the PIC. While in some configurations a polarization controller is not needed, in other configurations where it is included it can be set manually, or be electronically adjustable and advantageously not requiring resets to achieve an arbitrary polarization state (endless polarization controller).

Turning now to FIGS. **8**(*a*)-**8**(*c*), there it shows three examples of k-clock processing modules according to aspects of the present disclosure. And while three illustrative examples are depicted in FIGS. **8**(*a*)-**8**(*c*), those skilled in the art will appreciate that additional configurations are possible and contemplated. Generally, with respect to k-clocks, it is noted that in some embodiments—such as when a frequency sweep is very linear in time and repeatable—a k-clock is not needed. In other embodiments, a k-clock allows one to compensate for non-ideal frequency sweep parameters in the tunable laser. For example if the tunable laser is swept in a sinusoidal (or other waveform) sweep over time, then a k-clock will allow an output clock to be triggered at substantially regular frequency increment intervals and such signals will trigger the ADC (or be used in alternative digital signal processing if fixed time ADC sampling is used) such that a proper Fourier transform takes place. As discussed previously, structures according to the present disclosure advantageously integrate k-clock(s) into/onto the PIC along with a number of other optical and electrical functions.

With initial reference to FIG. **8**(*a*), there it shows a simple dual balanced embodiment where two 50/50 couplers and a differential path delay are used in combination with dual

balanced photo detectors. Turning now to FIG. **8**(*b*), there it shows a non-differential embodiment where there are two (I and Q) electrical optical and electrical outputs phase shifted by 90 degrees. Finally, FIG. **8**(*c*) shows an illustrative embodiment where there are two (I and Q) electrical optical and electrical outputs and each one of them contains a differential detection to eliminate common-mode noise. As noted previously, while these three illustrative embodiments are shown, those skilled in the art will understand that other embodiments are contemplated according to the present disclosure.

As may be appreciated, it is sometimes beneficial for the optical path length—such as that shown previously in FIGS. **1-7**—from the laser source to the sample and further to the photodetector(s) to have approximately the same total delay as the path from the laser source to the triggering of the ADCs via the k-clock processing module. One way to achieve this is to have an optical delay between the laser output and the k-clock input that matches both delay and dispersive properties of the two path lengths. If the delay is small enough (~1 cm) then it can be contained within the PIC. If the delay is much longer, then a fiber optical patch cord can be designed into the path between the 90/10 coupler and the k-clock input (not shown). Another alternative method to achieve the same total optical delay is to introduce an electronic delay buffer after the photo-detection. In particular configurations such as when the laser souse tuning characteristics permit, such an arrangement may be a preferred one. Finally with reference to FIG. **8**(*a*)-**8**(*c*), it is noted that clock generator and electrical processing elements may advantageously comprise TIAs, filters to reduce out of band noise, zero-crossing detectors, AGC elements, digital logic (e.g. OR, XOR) phase shifters, and dummy clocks and other processing functions. In still another alternate embodiment, the k-clock may comprise a ring resonator filter instead of a Mach-Zehnder interferometer.

As may be appreciated, one critical component of an SS-OCT system—as well as other optical systems—is the laser source. More particularly, a desirable laser source exhibits the following characteristics namely, rapidly tunable, widely tunable, stable, long-coherence length, desirable optical signal to noise ratio (OSNR), minimal excess intensity noise, compact, reliable, and inexpensive. It is also advantageous for such a laser source to exhibit a near sawtooth waveform in terms of wavelength (or frequency) vs. time.

FIG. **9**(*a*) shows one illustrative embodiment of a frequency tunable source according to an aspect of the present disclosure. As shown, the tunable source includes a seed laser, an optical switch, an amplifier, a frequency shifter, a tunable optical filter, an isolator and a polarizer—all configured in a common ring arrangement. Operationally, at the start of each laser sweep the optical switch is connected to the seed laser. This seed laser provides the necessary output power and coherence length sufficient to start the frequency sweep while preferably saturating the optical amplifier to minimize ASE noise. The seed laser can be integrated into the PIC or externally located and fiber coupled onto/into the PIC. The light from the seed laser is optically amplified and sent to the frequency shifter and is maintained long enough in the ring to stabilize the light and amplifier.

We note that there exist alternatives to the seed laser such as using a single frequency reflector in combination with the ring gain element to produce a laser starting frequency. Also in one embodiment the 2:1 switch and seed laser can be eliminated and the tunable optical filter is set to the starting frequency and the frequency shifter is turned off for a period sufficient for the ring laser to begin lasing on a ring cavity within the tunable optical filter bandwidth.

Notably, the illustrative embodiment depicted in FIG. **9**(*a*) is arranged as a unidirectional ring. Those skilled in the art will appreciate that other arrangements using linear cavities or alternative configurations are contemplated by this disclosure as well. More specifically, the ring arrangement may be fabricated within a single integrated optical component or particular part(s) of the ring arrangement may be external to the PIC (e.g. in optical fiber or free space).

Continuing with our operational discussion of the frequency tunable source depicted in FIG. **9**(*a*), at a particular time (preferably the round trip time), the switch is enabled and the light begins to circulate around the ring as depicted in the line chart. For each circulation around the ring, the light is shifted in frequency by f_Δ and this shift continues until the desired total sweep range is completed f_D. The total sweep time is completed in $1/f_s$.

As may be readily appreciated, there are several ways to generate a constant frequency shift. With reference to FIG. **9**(*b*), there it shows an illustrative example using a simple phase modulator that is reset at integer multiples of 2 π. FIG. **9**(*c*) shows another illustrative example to generate a constant frequency shift which employs two Mach-Zehnder modulators biased at their null point and driven in their linear range. The two modulators are similar but one input includes a 90 degree optical phase shifter. If the Mach-Zehnder modulators are operated in their linear regime, then the drive signals are sinusoids. If the Mach-Zehnders are driven to their full extent of +/−pi, then the drive signals are triangle waves.

Note that it is important to maintain stable operation of the frequency shifter and in particular to extinguish any unshifted, spurious harmonics of the input light. To maintain such conditions, automatic bias control circuits for biasing each modulator at its null position and adjusting the RF drive amplitude and phase can be implemented similar to those used for optical telecommunication systems such as DP-QPSK and other systems that use Mach-Zehnder modulators.

As noted previously, when the frequency tunable source is configured as a ring such as that shown, the ring may optionally include a polarizer to extinguish unwanted light as normally the ring runs in a single polarization. The optical gain may be provided by rare-earth (e.g. Yb/Er) doped waveguides; from monolithically integrated optical gain elements like InP, GaAs, Germanium, or III-V quantum dot material such as InAs; or using a wafer bonded or butt coupled optical gain elements such as InP or GaAs, or other semiconductor material either integrated with the PIC or external to a PIC that can be optically or electrically pumped. Similarly, frequency shifters may be fabricated in any of a number of optical compatible materials. Notably, if they are fabricated in Si, they may be either carrier injection or carrier depletion type modulators—or even both if they are modulators having an oxide in the junction.

Note that ring structure depicted in FIG. **9**(*a*) includes an optical isolator and a tunable optical filter. In an alternate embodiment(s) the isolator and/or tunable optical filter is/are not needed. This is particularly appropriate in those situations wherein the frequency shifter produces minimal carrier leak through and spurious harmonics and the number of circulations of the ring over a scan period is sufficiently small such that only modest amplified spontaneous emission (ASE) and harmonic noise builds up in the ring.

With further reference to FIG. **9**(*a*), it is noted that a tunable optical filter is employed. This tunable optical filter

is not always needed but for certain configurations, such as a large number of light circulations, it can be beneficial. Advantageously, it may be fabricated using a narrow filter with fine tracking or relatively coarse bandwidth filter with corresponding coarse tracking One advantage of the tunable filter is that it can suppress any residual ASE noise and spurious signals (such as unshifted light leaking through the frequency shifter) from building up in the laser cavity.

With this additional suppression of the tunable optical filter, the number of cycles of the loop can be increased and the cavity length decreased to the point where the entire laser is housed in a PIC. Additionally, a polarizer can be employed to eliminate unwanted ASE and light scattered into the orthogonal polarization (as indicated in FIG. **9**(*a*)). Notwithstanding, it is possible to use a gain element that supports one polarization and thus there is no need for an additional polarizer. Furthermore, an optical isolator may be incorporated to ensure unidirectional operation if needed. This isolator can be off the PIC or can be contained on the PIC. Also as mentioned above and shown in FIG. **9**(*a*), an alternative to the use of the optical switch is to use a fiber optic coupler and two on/off switches. Such an approach can be easier to control and implement at the expense of increased throughput loss.

Shown further in FIG. **9**(*a*) is a circuit for controlling the optical gain or output power of the optical amplifier (OA). For example, in constant-power mode, a small optical tap at the output of the OA is used to estimate the output power and this signal is fed back to internal parts of the OA (e.g. pump or VOA) to keep the output power constant. Other methods for power and gain control are known and contemplated as well.

Finally with reference to FIG. **9**(*a*), note that a constant frequency shift is illustrated in this figure. Notwithstanding, it is possible to adjust the frequency shift over time to account for slight variations in propagation delay around the loop with wavelength if desired.

FIG. **10** shows a graph of our measured example of the frequency shifter shown in FIG. **9**(*c*) in operation using a Si photonic I-Q modulator. This frequency shifter was created in a silicon photonic integrated circuit. The line shown in the center of the graph is some of the carrier leak through. The frequency shift is −15 GHz and the side mode suppression ratio (SMSR) is 15 dB. As may be appreciated, the performance of this frequency shifter may be improved with better electrical tuning however the figure clearly shows the functionality of the device.

With reference now to FIGS. **11**(*a*) and **11**(*b*), there it shows two additional embodiments of frequency shifter topologies for homodyne frequency tracking in telecommunication systems. With reference to FIG. **11**(*a*), the embodiment shown is a single side band (SSB) modulator. It comprises an I-Q modulator driven by two triangular waves having peak-to-peak amplitude of π and a 90° relative phase shift. Operationally, the output rotates endlessly around the origin of the complex plane with a linear change in phase with time.

As is known, SSB modulation is traditionally performed at a fixed frequency. One advantage of the embodiment of FIG. **11**(*a*) is the modulator is driven from a digital-to-analog converter (DAC) with a look-up table, and the driving frequency constantly varies as the table is read out at a speed proportional to the required phase shift rate. Notably, SSB modulators are traditionally made in LiNbO3 and designed to run at high speeds. In this application however, we wish to operate the SSB modulators at low speeds (<1 GHz) and in a silicon PIC. Advantageously, this allows us to use current injection rather than carrier depletion modulation, resulting in low optical loss and low drive voltages. Finally, an SSB modulator such as that depicted in FIG. **11**(*a*), exhibits a 6-dB excess loss.

FIG. **11**(*b*) on the other hand, shows a schematic SSB modulator design exhibiting only 3-dB excess loss. This design has the additional advantage of requiring only sinusoidal drive signals rather than triangular wave signals, which may be easier to generate. The design of FIG. **11**(*b*) exhibits lower loss because rather than using just 3-dB couplers on the input and output it uses Mach-Zehnder switches that redirect the distribution of light between the I and Q modulators as the phase progresses around its circle. These are driven with twice the frequency as the I and Q modulators but only ~1/13 of the amplitude.

FIG. **12** shows one of many possible examples of a tunable filter that can be driven in a sinusoidal or preferably a digital fashion to minimize degradation in the output laser quality due to build up of ASE and/or spurious harmonics in the laser loop. (Note that in this disclosure we may refer to this loop as a laser loop even though in some embodiments there is not laser action and the cavity operates more like a long transmission line). The basic concept is that of a Mach-Zehnder modulator with unequal path lengths. The path length difference is chosen to be such that the transfer function has a transmission null at one f_Δ above and below the desired frequency shifted carrier and at all the subsequent periodic nature of the transfer function. These are qualitatively illustrated by the "X's" on FIG. **12**. On the even trips one (blue) transfer function is applied. On the odd cavity trips the other (red) transfer function is applied. It is important that the modulator be driven rapidly so as to avoid collapsing the signal amplitude due to repeatedly passing through the modulator (similar to "eye closure" in digital communication signals). This modulator can have automatic bias circuitry that control the bias point (at null) and controls the relative amplitude and phase of the RF square wave or sine wave drive signal. Note the filter of FIG. **12** works well when driven in a wide bandwidth square wave fashion. And while it is also possible to drive the modulator with a sine wave which need not have a broad bandwidth, this can result in more distortion of the ideally constant amplitude signal but has the advantage of easier RF drive requirements.

To address the fact that the periodic power transfer function of the Mach-Zehnder filter may not ideally follow the constant frequency increment of the laser over a 100 nm or more sweep it is possible to utilize a more intelligent waveform than a simple sine or square wave to account for keeping the carrier at the center of one of the periodic peaks of the Mach-Zehnder transfer function at all times. Advantageously, it is also possible to alter the frequency of the frequency shifter.

Advantageously, it is possible to use more than one stage of Mach-Zehnder filtering. There are a variety of modulator delay configurations that can be used and the basic concept is to place nulls of each stage to eliminate spurious leak though of the carrier and unwanted harmonics. In many applications it suffices to have one stage. In other applications where a large number of cavity sweeps is desired two or more stages can be used. In order to drive the Mach-Zehnder modulator properly one approach is to provide a high-speed multi-channel DACs closely coupled to the Mach-Zehnder modulators. To keep the Mach-Zehnder path lengths short and within a single PIC it is beneficial to include a high frequency shift in the ring (e.g. 10 GHz).

Note that gain sections for tunable optical sources according to the present disclosure may comprise semiconductor

optical amplifiers (SOAs), doped waveguide amplifiers, wafer bonded gain elements on silicon wafers, InP regrowth, germanium doped silicon lasers, or doped fiber amplifiers. It is also possible to configure multiple gain sections in parallel using WDM or other splitting/combining techniques to broaden the bandwidth. That is to say one could use multiple SOAs (or other gain mediums) in parallel connected in phase and with equal path lengths but different gain spectrum peaks.

In another alternative tunable laser embodiment according to the present disclosure are one(s) in which there are two or more frequency shifters in the laser cavity as, for example, shown in FIG. **13**. Such an embodiment operates analogous to a Vernier laser cavity in which the light is split between two resonant cavities with different free-spectral ranges. Only certain cavity modes line up in both cavities simultaneously acting like an intracavity filter.

In one embodiment of this the rate of change of the frequency shifter is less than the cavity round trip time. In this structure is a laser undergoing laser oscillation and so the frequency sweep could be as slow or fast (the sweeping in one preferred embodiment is slow compared to the round-trip time) and there is much less concern about degradation in the buildup of amplified spontaneous emission (ASE) noise and subsequent reduction in optical signal to noise ratio (OSNR) of this approach due to its laser cavity characteristics than other approaches. The sweep in this embodiment could be continuous or it could be stepped. DACs (not specifically shown) can be used to directly drive the frequency shifters.

One interesting aspect of this embodiment is that these I-Q modulator types of frequency shifters are fundamentally different than acousto-optic frequency shifters in that the laser light adiabatically jumps back cavity modes as the laser is swept in frequency. Advantageously, seed lasers, tunable optical filters, isolators and other elements can be added to this cavity to improve operation at the expense of complexity. FIG. **13** shows two frequency shifters in parallel however, more or less could be used. More frequency shifters configured in parallel can produce a better rejection of unwanted cavity modes and the expense of increased complexity and wafer yield issues.

FIG. **14** shows yet another embodiment of a tunable optical source according to an aspect of the present disclosure. More particularly, FIG. **14** shows a schematic block diagrams illustrating a ring laser configuration having a frequency shifter and an optional tracking filter wherein the frequency shifter is configured to shift light entering into it to a new frequency that is closely aligned with a ring cavity mode. In this embodiment the frequency shifter is driven at a rate approximately equal to the round trip frequency (1/(round-trip-time)) or a multiple of the round trip frequency. In this fashion the light remains more coherent as it propagates around the cavity, and thereby suppresses ASE noise buildup and at each circulation the frequency is incremented and this results in a step wise sawtooth frequency sweep. An optional isolator can be included in the cavity but in a number of embodiments it is not needed.

The laser depicted in FIG. **14** may benefit from a tunable tracking filter to extend the tuning range and to keep unwanted cavity modes from building up in power. In other embodiments—particularly where smaller optical frequency sweep is needed—no tracking filter is needed.

Shown as an illustrative example, in the lower right hand corner of FIG. **14** there is the optical amplifier gain spectrum, the ring cavity modes, and the tracking filter. In one embodiment the tracking filter has a finesse of ~100, a bandwidth of ~1 nm, and a tuning speed of 10 MHz. There are a variety of other embodiments that are possible. Note that it may be highly beneficial that the tracking filter be synchronous with the cavity mode hoping from mode to mode.

As is known, chromatic dispersion and non-linear tuning of the filter can cause it to become slightly misaligned. It is possible to adjust the frequency shifter drive frequency and/or the tuning rate of the filter so they remain properly aligned. The seed laser can be connected by an on/off switch and a coupler, a 2:1 optical switch, or the seed laser itself can be turned on or off directly. Such a laser can be aligned to one of the lower cavity modes and have the proper power and coherent length characteristics suitable for the imaging application. The laser can be directly turn on/off at the start of the sweep or the laser can be left on to achieve stable operation and a separate on/off modulator can be use.

As noted above, to account for slight changes in the round-trip-time as the laser is scanned in frequency the frequency shifter frequency can be slightly adjusted in time to ensure that the shift of the light remains at or near a cavity resonance mode.

If the frequency shifter depicted in FIG. **14** is constructed using the approach described previously with respect to the configuration of FIG. **9**(*c*), then it is possible to alter the function of the device "on the fly". That is, the device of FIG. **9**(*c*)—with the addition of the normal electrically adjustable phase trims (not specifically shown)—can advantageously implement a variety of intensity and phase modulation waveforms.

For example it is possible to slowly or rapidly change the modulation format from "pass through mode" (e.g. no intensity or phase modulation) to frequency shifting mode. One advantage of this type of operation is it is possible to let the laser light circulate more than one round-trip-time within the laser cavity. This has the further advantage of allowing the sweep rate to be decreased (for more SNR during data collection) and allows the laser light to increase its coherence and settle for a longer time into the proper laser cavity mode. One additional benefit of this approach is that the laser sweep rate can be reconfigured on the fly to integer multiples of the fundamental sweep rate.

A basic idea behind this operation is that the laser operates at a cavity mode for one or more round-trip times. Then it is desired to move to a new cavity mode. Instead of just tuning a filter and restarting the laser at the new cavity mode and waiting for light in the laser cavity to build up from ASE and other noise sources, the new laser cavity mode is seeded with a strong light signal from the previous cavity mode. This has the benefit of improving both the coherence of the light and the rate at which the laser cavity can be tuned.

Note that with configurations such as those depicted in FIG. **14** there are various types of tracking filter that can be used including a single or multiple set of coupled ring resonators, Mach-Zehnder, Fabry Perot, and grating filters. As noted, it is possible to use no tracking filter at all specially for relatively short sweep ranges.

With reference now to FIGS. **15**(*a*) and **15**(*b*), there they show alternate embodiments of a reconfigurable laser modulator that exhibits a state of either frequency shift or pass-through. The top path in each FIGS. **15**(*a*) and **15**(*b*) includes a frequency shifter. The bottom path includes a path length and loss trimming and matching fiber and other electro-optical characteristics that can be matched to the upper path. FIG. **15**(*a*) shows an example configuration wherein on/off modulators are used along with passive couplers. FIG. **15**(*b*) shows an example wherein 1:2 and 2:1

optical switches are used. Such switches can be Mach Zehnder or other types of integrated optical switches.

At this point it is notable that it may be beneficial to use silicon photonics for much of the PIC fabrication and couple another type of electrically or optical pumped optical gain medium that is configured to work in a double pass geometry through a gain medium. A double pass gain geometry can be beneficial in embodiments where the majority of the PIC is a single silicon photonic integrated circuit and that PIC is butt coupled (or otherwise coupled) to an InP or other material optical gain medium. It is possible to use a beam splitter and a double pass amplifier (where one facet of the amplifier is HR coated) instead of a unidirectional amplifier. Another approach is to use a combination of half wave plate and quarter wave plates and a polarization beam splitter to allow for more efficient operation. However such polarization isolation approaches require the gain medium be able to support both polarizations.

FIG. **16** shows an example of an embodiment of a tunable laser wherein the frequency shifter operates in a linear cavity (not a ring configuration) and a gain medium operates in a double pass geometry. High speed DACs can be directly coupled with the tuning elements to ensure rapid, high-speed agile tuning.

With reference now to FIG. **17**(*a*), there it shows linear cavity examples of tunable lasers that do not employ a frequency shifter modulator. When there is no frequency shifter, in one exemplary embodiment the laser mode hops as it tunes. In other alternative exemplary embodiments cavity length adjustments may be made along with other approaches to minimize mode-hopes. It yet another exemplary embodiment the laser operates in several laser modes at once (e.g. multi-mode) and the groups of different modes are active as the nominal laser frequency is tuned.

FIG. **17**(*b*) shows an exemplary embodiment employing one ring resonator and FIG. **17**(*c*) shows another exemplary embodiment where two ring resonators are employed. In a preferred embodiment of the embodiment of FIG. **17**(*c*), the ring resonators have different free spectral ranges and the two rings operate in a vernier tuning mode to extend the tuning range of the laser beyond that possible with just one ring resonator.

FIGS. **18**(*a*)-**18**(*b*) shows an example of a complete photonic integrated circuit similar to some of the systems shown in previously. The receiver portion is a dual polarization I/Q dual balanced configuration similar to those shown in FIGS. **4**, **5**, and **6**. This particular illustrative embodiment uses a silicon photonic PIC with a recessed region that contains an InP two-channel optical gain element. One side of the InP gain element contains HR coatings and the other side (which interfaces with the SiPh PIC) contains angled facets to minimize any unwanted reflections. As described earlier an alternative to this butt coupled InP gain element approach shown in FIG. **18**, other types of but coupled gain elements other than InP can be used and furthermore it is possible to monolithically integrated the gain on the PIC substrate (and not use butt coupling) by using known approaches such as growth of III-V quantum dots (e.g. InAs), Germanium, or InP or by using wafer bonding approaches and evanescent or other optical coupling of the light from the silicon photonic circuit into the bonded optical gain element. The optical gain elements can be optically or electrically pumped.

In this embodiment there are two separate gain elements in the InP chip that contain gain peaks at different wavelengths. In this manner it is possible to have an optical frequency sweep that is broader than one gain element can provide. In another embodiment (not shown) one element is used instead of two for simplicity. In other embodiments there could be more than two gain elements for even broader frequency sweeping. At the output of the upper gain element there is a phase shifter. This phase shifter can be thermal or electro-optically tuned.

One purpose of this phase shifter is to match the nominal optical path lengths such that in spectral areas where the laser light has significant components from both gain elements the light from each gain element constructively combines in the coupler. One purpose of the Mach Zehnder combiner (M/Z Combiner) is to optimize coupling of light to the upper gain element or the lower gain element. For example when the laser is operating at a wavelength aligned with the peak of the lower gain element this M/Z would have a null at the upper gain element gain peak. At a laser wavelength aligned with the peak of the upper gain element the M/Z would have a null in transmission at the lower gain peak. This M/Z could also contain adjustable phase shifter elements (not shown) to allow for active alignment. There are other combinations of M/Z filtering functions and gain peak arrangements that are possible.

Operationally, the laser depicted in FIGS. **18**(*a*)-**18**(*b*) operates in a manner similar to that shown in FIG. **13** in that two frequency shifters are utilized and driven at different rates but the laser is in a Michelson interferometer embodiment instead of a ring cavity laser configuration. There are two frequency shifters and the outputs of the frequency shifters are connected to loop mirrors and thus the frequency shifters operate in a double pass configuration. Note that this laser embodiment could be replaced with the other laser embodiments as described elsewhere in this document. This includes a single frequency shifter approach, a single frequency shifter with a tunable tracking filter, and a tunable laser with no frequency shifter at all. One could employ more or less frequency shifters than shown in FIGS. **18**(*a*)-**18**(*b*).

Note that while FIGS. **18**(*a*)-**18**(*b*) do not explicitly illustrate a seed laser, those skilled in the art will recognize that an integrated or external seed laser with appropriate interconnect may be incorporated into the structure(s) shown therein according to aspects of the present disclosure. Alternatively, and as discussed previously, there are ways to eliminate the need for a seed laser by incorporating wavelength selective optical elements.

The PIC output couplers and PIC input couplers are surface grating couplers and may be similar to those shown previously in FIG. **5** except that in FIG. **18**(*a*), only one PIC output surface grating coupler (SGC) port is used and the reference and sample probe light splitting is done external to the PIC. FIG. **18**(*b*) shows an alternate embodiment for the Probe out and the Ref out that has a 90/10 splitter and two 1D output grating couplers on the PIC.

The reference input coupler is a 1D surface grating coupler and leads to two multi-mode interference (MMI) couplers to provide for X and Y polarization. The probe input coincides of a 2D surface grating coupler with normal fiber incidence. Each of the two common polarization arms are couple via a phase shifter and nearly 50/50 coupler into a common optical path and then coupled to the MMI couplers. The output of each MMI coupler consists of two differential outputs that form a dual-balanced I/Q receiver. The unused ports of the near 50/50 couplers can be used for power monitoring. An alternative to using a 2D normal incidence surface grating coupler is to use a 2D non-normal incidence coupler.

With reference now to FIG. **19**, there it shows another illustrative embodiment according to the present disclosure that uses facet couplers instead of the surface grating couplers shown in FIG. **18**(*a*). One benefit of facet couplers is they can achieve both low loss and very broad coupling bandwidth at the expense of fabrication and alignment complexity and the requirement for a planar polarization splitter and rotator. To achieve polarization rotation and splitting then the facet couplers are followed by integrated polarization beam splitters and integrated polarization rotators (PBSR) in the probe arm input channel. To achieve a long delay with low loss in the long arm of the k-clock (e.g. 2-20 mm) SiN, SiON, or other waveguide structures can be used. Also shown in FIG. **19** is a seed laser that contains a fixed (or tunable) Bragg grating reflector. This seed laser and be turned on and off by applying electrical current to the gain medium. The seed laser can be used to start the initial conditions of the frequency sweep in the laser cavity. The seed laser is optional.

For very broad coupling bandwidth, one can use facet couplers with spot-size converters as shown in FIGS. **19**, **20**, and **21**. If these facet couplers are used instead of the 2D grating couplers, then the facet couplers must be followed by integrated polarization beam splitters and integrated polarization rotators in one output of the polarization beam splitters (PBSR).

An integrated polarization beam splitter can be, for example, a direction coupler in silicon wire waveguides that is 100/0 coupling for TM and nearly 0/100 for TE. A polarization rotator can be, for example, an adiabatic transformation that uses asymmetric waveguide structures/placements to achieve significant mode splitting when the waveguide modes are hybrid TE/TM modes.

Note in both FIGS. **18**(*a*)-**18**(*b*) and **19** it is possible to configure using another embodiment that only has one frequency shifter in series with a tunable optical filter, or no frequency shifter at all and just tunable optical filters. It is also possible to add in PIC optical isolators using couplers and phase modulators.

FIG. **20** shows another illustrative embodiment integrated onto a SiPh PIC including with a widely tunable laser using tunable filters. As may be observed, a Mach-Zehnder interferometer (MZI) switch switches between two ring-resonator-based tunable filters. The ring resonators are Vernier tuned.

The tuning works as follows. The MZI sends the light to the upper tunable filter. The upper filter begins to tune from one end of the gain spectrum to the other. When the phase tuners in the rings run out of adjustment range, the second filter is adjusted to be at the same wavelength as the upper filter and same phase but using phase tuners set at the beginning of their ranges. The switch then switches and the lower filter tunes and the phase tuners in the upper filter reset.

When the lower filter exceeds its adjustment range, the switch switches back to the upper filter and the overall process continues. As may be appreciated, this type of swept laser may experience mode hops as the wavelength is tuned. However, phase tuners may be positioned in each ring resonator section such that they remain in a cavity mode and the switch operates every time one of these phase shifters exceeds its normal range. In this way the frequency sweeping could be mode-hop free or with reduced mode-hops. In order to be near mode-hop free, as the switch switches, the relative phase between the two paths is adjusted be zero, so that during the switching, which necessarily takes a finite amount of time, the laser does not mode hop. Also, other tunable filters could be substituted for these double-ring resonator structures.

Alternatively, if one does not care about the presence of mode hopping during tuning, then one could eliminate the switch and just one Vernier-tuned ring resonator set. In this case, one possibility is to drive the two ring resonators with programmed voltages via digital-to-analog converters so that the wavelength sweep is monotonic across the band. There would likely be mode hopping because the ring voltages would have to be non-monotonic and would have to reset at times. An alternative possibility is to drive one ring with a monotonic voltage waveform, leaving the other one substantially constant. This would cause the wavelength to tune in discrete steps. After this sweep of one ring, then the second ring could be adjusted a small amount and then the first ring swept again. This would allow one to eventually cover all the wavelengths in the band, but in a non-monotonic, moving-comb fashion. Post detection reordering of the frequency samples in a DSP unit could be used to perform the FFT.

In yet another illustrative embodiment of the structures depicted in FIG. **20** it is possible to use just one gain element in the gain chip thereby eliminating the M/Z combiner and reducing fabrication complexity at the expense of tuning range. It is also possible to reduce fabrication complexity and cost to use just one set of tunable filters and thus eliminate the M/Z switch in applications that require less tuning speed and tuning range.

Yet another illustrative embodiment according to the present disclosure is shown schematically in FIG. **21**. In this illustrative embodiment shown in FIG. **21** there is a single frequency shifter and a tunable tracking filter constructed using a length-imbalanced Mach Zehnder interferometer having a large free-spectral range. As may be readily appreciated, a large free-spectral range makes tracking easier. A narrower band tunable tracking filter can be used but requires a more complicated filter structure if it is desirable to tune the whole frequency band without any resets. Also there is one output fact coupler/spot-size converter for the probe and reference outputs which are then split using an external splitter.

Yet another illustrative embodiment according to the present disclosure is shown schematically in FIG. **22**. It contrast to the structures depicted in FIG. **21**, the structure(s) of FIG. **22** includes a dual-polarization arbitrary I/Q modulator comprising out of phase shifters, splitters, combiners, and a Mach-Zehnder modulator. The various phase shifters are for adjusting optical path lengths and may be carrier depletion, or other types of modulators and may be thermal or electro-optically activated. The outputs of the two modulators are combined in a PBSR and it is also possible to use simpler absorptive types of modulators at the expense of higher loss. Other types of modulators are possible such as fast VOAs.

FIG. **23**(*a*) shows an illustrative example schematic of silicon PIC according to an aspect of the present disclosure. A receiver portion comprises a single-polarization dual-balanced I/Q receiver similar to that shown previously in FIG. **3**. The PIC delay is included within the PIC. A laser contains InP gain chip butt coupled to a silicon photonic integrated circuit similar to that shown in FIGS. **18**-**22**. The laser cavity includes of two Vernier tuned ring resonators, a fast phase tuner element, and a single loop reflector. The output waveguides are coupled to a facet coupler labeled "output" which further coupled to a single mode optical fiber. FIG. **23**(*b*) shows a photograph of the device. FIG.

23(c) shows the output laser tuning characteristic over ~4.8 THz. Wider wavelength tuning is possible.

Note that the structures depicted in FIGS. 18-23 show an optical gain chip set into a silicon photonics PIC. There are a variety of other methods to add an optical gain compatibility with a silicon substrate such as using wafer bonding, regrowth, or directly doping the silicon PIC with germanium or rare earth dopants to provide gain. Furthermore it is possible to build the entire PIC out of another optically compatible medium such as InP, InAs, GaAs, GaAlAs, InGaAs, or many other optically compatible semiconductor materials. For example, it has been demonstrated that InAs quantum dot (QD) lasers can be applied directly to silicon to produce optical gain in the 1.3 um region. Some of these cited approaches can have the benefit of providing gain in one medium but the disadvantage of being less compatible with the silicon processes commonly used in semiconductor foundries.

To couple from a PIC to either a fiber or free space optics, a broadband low-loss coupling is needed. As discussed earlier, two common methods to achieve this are surface grating couplers and fact coupling (also referred to as end-coupling or butt-coupling). Such coupling is needed at the interfaces from the integrated components (dotted lines in FIGS. 2-7 and in the Probe out, Ref Out, Probe In, and Ref In of FIG. 18-23) or wherever there are input/output locations where light travels on or off the PIC.

Coupling may also be needed—as discussed earlier—if the swept source laser contains optical path lengths in fiber, and/or if the increased delay is needed between the 9/10 coupler and the k-clock input. As discussed earlier in some particular embodiments PIC surface grating couplers are used and in other embodiments facet/end/butt coupling is used. To achieve a robust and manufacturable system, it is convenient to place multiple fibers (2, 3, 4, or more depending on the system requirements) in a single glass block that is precisely manufactured to have the same dimensional separation between fibers as the separation of the PIC inputs and outputs. The fibers can be housed and secured in the glass block using epoxy and polished as a unit to ensure low-loss coupling. A manual or automatic multi-axis machine can be used to align the glass block to the fiber waveguide interfaces on the PIC. FIG. 24 shows and example of a low loss fiber assembly housing three single mode optical fibers coupled to a silicon photonic circuit containing modulators and receiver that we have constructed.

A PIC may be housed our otherwise contained in any of a number of optical mechanical packages known in the art. However it is highly beneficial if the PIC is closely integrated with the transimpedance amplifiers (TIA) and that both are contained in one package. There are several methods for achieving this proximity as shown in FIGS. 25(a)-25(c) which depict co-packaging of the PIC and electronics. FIG. 25(a) shows the PIC mounted in a ceramic or metal package, wirebonded with TIAs and driver circuits. The driver circuit may contain modulator drivers, phase shifter drivers, thermal drivers, and DACs, among other components.

Alternatively those active electrical components may be located external to the package. FIG. 25(b) shows an example where the PIC is co-packaged with the TIAs and a digital circuit such as an ASIC, FPGA, or other mixed signal electronics.

FIG. 25(c) shows an example embodiment in which the TIAs are further integrated with an application specific integrated circuit (ASIC). Wire bonds, die bonds, wafer stacking, and other approaches can be used to optically, mechanically, and electrically interface with the PIC.

FIG. 26 shows an illustrative example where the PIC and ASIC are die bonded to a substrate that may comprise silicon, FR4, or another suitable substrate carrier that also contains ball bonds. It is possible to replace the substrate ball bonds with leads or pins in alternate embodiments. The substrate carrier could be active or passive device. Also shown is a metal cover and heat sink and thermal coupler to connect the top of the ASIC to the cover and heat sink.

At this point those skilled in the art will readily appreciate that while the methods, techniques and structures according to the present disclosure have been described with respect to particular implementations and/or embodiments, those skilled in the art will recognize that the disclosure is not so limited. In particular, where multiple integrated chips are employed, those chips may advantageously be closely coupled by positioning them on a common carrier or within a common packaging. As may be appreciated, in this manner the chips may be physically close to one another of close in time to one another as appropriate. Accordingly, the scope of the disclosure should only be limited by the claims appended hereto.

The invention claimed is:

1. An optical system for optical coherence tomography comprising:

interferometer circuitry configured to divide a tunable optical signal between a reference path and a sample path and to combine optical signals returning from the reference path and the sample path to generate an interference signal, said interferometer circuitry including dual-polarization, dual-balanced, in-phase and quadrature (I/Q) detection outputs;

a detection system comprising at least one photodetector coupled to the interferometer circuitry; and

a tunable optical source configured to generate the tunable optical signal;

wherein the interferometer circuitry and the tunable optical source are integrated onto a photonic integrated circuit (PIC).

2. The optical system of claim 1 further comprising a k-clock module configured to generate a k-clock signal for triggering the detection system, wherein said k-clock module is integrated onto the PIC.

3. The optical system of claim 1 wherein said tunable optical source includes one or more optical frequency modulators.

4. The optical system of claim 1 wherein said tunable optical source includes one or more tunable optical filters.

5. The optical system of claim 1 further comprising one or more surface grating couplers integrated onto the PIC and configured to couple light between the PIC and one or more optical fibers.

6. The optical system of claim 1 further comprising one or more facet couplers integrated onto the PIC and configured to couple light between the PIC and one or more optical fibers.

7. The optical system of claim 1 further comprising a non-silicon optical gain element in optical communication with the PIC, wherein the PIC is a silicon photonic PIC.

8. The optical system of claim 1 wherein the PIC includes a plurality of optical ports, and wherein each one of said plurality of optical ports is coupled to an optical fiber, and each one of said optical fibers is included in a single block affixed to the PIC.

9. The optical system of claim 1 further comprising a carrier substrate onto which is mounted the PIC and one or more additional electrical chips.

10. The optical system of claim 1 further comprising an optical gain element integrated onto the PIC, the optical gain element having a gain response that is wavelength-dependent.

11. The optical system of claim 1 further comprising a modulator integrated onto the PIC, said modulator positioned in an optical path of the tunable optical signal.

12. The optical system of claim 1, further comprising processor circuitry configured to process the interference signal to determine information about a longitudinal reflectivity profile of optical properties of a sample positioned in the sample path.

13. The optical system of claim 1, wherein the detection system is integrated on the PIC.

14. An electro-optical system comprising:

one or more couplers configured to optically couple light comprising a tunable optical signal into one or more photonic integrated circuits (PICs);

interferometer circuitry configured to divide the tunable optical signal between a reference path and a sample path and to combine optical signals returning from the reference path and the sample path to generate an interference signal; and

a detection system configured to detect the interference signal,

wherein the interferometer circuitry, one or more couplers and detection system are all integrated onto the one or more photonic integrated circuits (PICs) and commonly packaged or positioned on a common substrate.

15. The system of claim 14 where the interferometer circuitry comprises dual-balanced, in-phase and quadrature detection outputs and the detection system comprises integrated photodetectors.

16. The system of claim 14 where the interferometer circuitry comprises dual polarization, dual-balanced, in-phase and quadrature outputs and the detection system comprises integrated photodetectors.

17. The system of claim 16 further comprising a tunable optical source configured to generate the tunable optical signal and a k-clock module configured to generate a k-clock signal for triggering the detection system, wherein the k-clock module, the interferometer circuitry, the tunable optical source and the detection system are all integrated onto the one or more photonic integrated circuits (PICs).

18. The system of claim 14, further comprising processing circuitry configured to process the interference signal to determine a ranging or longitudinal reflectance image of a sample positioned in the sample path of the interferometer circuitry.

* * * * *